Methanol to Olefins (MTO): From Fundamentals to Commercialization

Peng Tian,[†] Yingxu Wei,[†] Mao Ye,[†] and Zhongmin Liu*[,†,‡]

[†]National Engineering Laboratory for Methanol to Olefins, Dalian National Laboratory for Clean Energy, Dalian Institute of Chemical Physics, Chinese Academy of Sciences, Dalian 116023, China

[‡]State Key Laboratory of Catalysis, Dalian Institute of Chemical Physics, Chinese Academy of Sciences, Dalian 116023, China

S *Supporting Information*

ABSTRACT: The methanol-to-olefins (MTO) reaction is an interesting and important reaction for both fundamental research and industrial application. The Dalian Institute of Chemical Physics (DICP) has developed a MTO technology that led to the successful construction and operation of the world's first coal to olefin plant in 2010. This historical perspective gives a brief summary on the key issues for the process development, including studies on the reaction mechanism, molecular sieve synthesis and crystallization mechanism, catalyst and its manufacturing scale-up, reactor selection and reactor scale-up, process demonstration, and commercialization. Further challenges on the fundamental research and the directions for future catalyst improvement are also suggested.

Methanol to Olefins
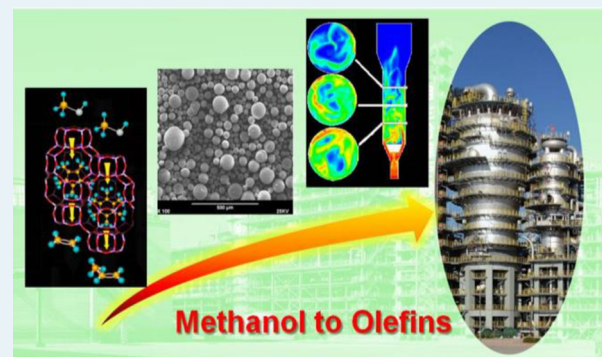
1. INTRODUCTION

The methanol-to-olefins (MTO) reaction is one of the most important reactions in C1 chemistry, which provides a chance for producing basic petrochemicals from nonoil resources such as coal and natural gas. As olefin-based petrochemicals and relevant downstream processes have been well developed for many years, MTO is believed to be a linkage between coal or natural gas chemical industry and modern petrochemical industry. Many institutions and companies have put great effort to the research of MTO reaction since it was first proposed by Mobil Corporation in 1977,[1] and significant progress has been achieved with respect to the reaction principle,[2−10] catalyst synthesis,[11−15] and process research and development (R&D).[16−19]

Methanol, which is very sensitive to a catalyst due to its high activity, could be catalyzed by acidic zeolites to form hydrocarbons. The reactant molecule is small and simple, but the reaction has been demonstrated to be very complicated with a large variety of products over different zeolite catalysts. The successful development of a commercially applicable MTO technology needs to solve many scientific and technical problems: (1) to establish a selectivity control principle for this complex reaction system through a deep understanding of the mechanisms of reaction and deactivation; (2) to develop an efficient catalyst through the application of new zeolitic materials and the study of interplay between synthesis method, catalyst property, and reaction performance; (3) to scale up the synthetic process of the catalyst with commercially available raw materials and establish standards to ensure the reliability and

repeatability for large scale catalyst production; (4) to find out a suitable reactor type with optimal reaction conditions and explore the commercial availability; (5) to make a complete process flow diagram and set up a reliable reactor scale-up approach; (6) to integrate the knowledge obtained from reactor scale-up with existing industrial experiences to make basic design package for commercial unit. There are many interesting results and excellent reviews on MTO reaction and process, which, however, mainly focus on the fundamental research.[2,3,6,20]

The Dalian Institute of Chemical Physics (DICP) has been dedicated to the R&D of the MTO reaction for more than 30 years, aiming at the development of a commercially available process technology.[21,22] Based on DICP's MTO technology, namely, dimethyl ether or methanol-to-olefin (DMTO), the world's first MTO unit was constructed and started up in August 2010 in Baotou, China, which is considered as an important milestone and critical step for producing light olefins from coal. In this historical perspective, we would like to share some of our research and experiences in the development of DMTO technology in DICP related to the aforementioned problems, from the fundamental research, catalyst synthesis, and process development to commercialization. We wish this perspective might shed some light on how the fundamental research of catalysis in the laboratory, via the multidisciplinar

collaborations, can be eventually developed into a commercial technology.

2. HISTORICAL DEVELOPMENT OF MTO IN DICP

The MTO research in DICP began in 1982 as a project supported by Chinese government and Chinese Academy of Sciences due to the concerns about the shortage of oil supply because of the oil crisis in the late 1970s. Two research groups were involved in the early researches, and one was in charge of zeolite synthesis and the other focused on zeolite modification and catalyst development. Based on ZSM-5 type catalyst, with participation of third research group, DICP finished a 300 t/a MTO fixed bed pilot plant test in 1993. In the meantime, following the findings of excellent MTO performance over small pore molecular sieves such as SAPOs and the idea that synthesis of dimethyl ether is more favorable in thermodynamics than that of methanol, we proposed a syngas via dimethyl-ether-to-olefins (SDTO) method in early 1990s.[22] In this process, the modified SAPO-34 catalyst was used to convert dimethyl ether to light olefins in a fluidized bed reactor. A pilot scale test on SDTO was finished in 1995. The SDTO results indicated that they met the expectation; however, it was still less economically competitive compared to the oil route at the time of low oil price. The MTO research in DICP then focused on molecular sieve synthesis and modifications in order to further improve the catalyst performance, which led to the development of DMTO technology.

In 2004, the DICP had a chance to demonstrate the MTO process at a large scale by collaborating with SYN Energy Technology Corporation and SINOPEC Luoyang Petrochemical Engineering Corporation. The latter is a well-known engineering company in China. DICP spent two years in scaling up the catalyst manufacturing and constructing a demonstration unit with a methanol feed rate of 16 kt/a.

The successful running of the demonstration unit not only provided the basic design data for the commercial units design but also encouraged the rapid industrial applications of DMTO technology in China. Up to now, seven DMTO units have been commissioned and put into stream.

3. FUNDAMENTAL STUDY ON MTO REACTION

MTO is an autocatalytic reaction,[23,24] in which the initial formation of a small amount of products leads to an enhanced methanol conversion until the efficient production period is reached. How C−C bond forms from C_1 reactant has been debated in the past decades. Early studies proposed many direct mechanisms to explain C−C bond formation from methanol or dimethyl ether, such as carbene mechanism,[1,25,26] oxysonium ylide mechanism,[27,28] carboncation mechanism,[24,29] free radical mechanism,[30,31] and so on, which were later proved energetically unfavorable by theoretical calculations. Over fresh catalyst, the slow kinetic rate of the initial methanol conversion implies that C−C bond formation during this period possibly goes through the reaction route with relatively high energy barrier. Until now, how the first C−C bond generates is still a controversial issue.

Some work in the early 1980s proposed the indirect pathway of olefins generation. Dessau and co-worker[32,33] suggested the alkene-based pathway, and Mole and co-workers[34,35] noted the profound influence of aromatics and suggested the aromatic cocatalysis in the generation of olefins. In 1993−1996, the hydrocarbon pool (HCP) mechanism was proposed by Dahl

and Kolboe,[34−38] i.e., cyclic organic species confined in the zeolite cage or intersection of channels act as cocatalysts for the assembly of olefins from methanol. The nature of HCP species has been investigated by several groups,[3,4,20,39−42] and intensive studies have proved that methylbenzenes are the HCP species in MTO reaction on SAPO-34 and revealed the correlation between the presence of methylbenzenes in SAPO-34 cages and the formation of olefin products,[5,43−48] in which Xu and White were the first to determine the structure of HCP species in an eight-membered ring molecular sieve catalyst.[41,42] With the aid of solid-state NMR spectroscopy, some carbenium ions have been identified as intermediates confined within zeolite catalysts, such as 1,3-dimethylcyclopentadienyl cation, indanyl cation, and 1,1,2,4,6-pentamethylbenzenium cation within HZSM-5; heptamethylbenzenium cation within H-beta, and heptamethylcyclopentenyl cation within SAPO-34.[49−53] However, the formation of most of these carbenium ions during methanol conversion was proved via indirect ways. The direct observation of such HCP species and their roles in methanol conversion over zeolites or SAPO catalysts under real working conditions is still a big challenge.

Two distinct reaction routes, the side-chain methylation mechanism and the paring mechanism, have been proposed to explain the MTO reaction pathway according to the HCP mechanism.[34,35,54,55] For the two reaction mechanisms, carbenium ions and their deprotonated counterparts are involved and act as the important reaction intermediates for olefin production.[9,48,56−59] Specifically, the paring route involves the contraction of six-membered ring ions (polymethylbenzenium cations) and the expansion of five-membered ring ions (polymethylcyclopentenyl cations). In contrast, the side-chain methylation route proceeds via the methanol methylation on polymethylbenzenium ions and subsequent elimination of side chain groups to produce olefins. The observation of carbenium ions and the explanation of the olefin generation from such intermediates present two essential questions in HCP mechanism study.

The aromatics-based hydrocarbon pool mechanism is important for cage type SAPO and H-beta zeolite with required space for the formation and function of the bulky HCP species.[44,46−48,54,55] In 2006, dual-cycle concept was suggested to explain the difference of the formation of ethene and higher olefins over H-ZSM-5.[7,60,61] It is suggested that ethene generation over H-ZSM-5 is related to aromatic-based HCP mechanism, and the propene and higher olefins formation follows an olefin methylation and cracking route.

For the deactivation of MTO catalysts, external coke formation is responsible for the deactivation of ZSM-5 by poisoning active sites or blocking pores.[62] Due to the narrow pore opening and big supercage, methanol conversion over SAPO-34 is characteristic of very quick coke formation and residue in the cage. Haw and co-worker[4] reported that during methanol conversion, methylbenzenes, the most active confined organics, formed in the cage of SAPO-34 are converted with time on stream to methylnaphthalenes and polyaromatics, phenanthrene derivatives and pyrene, the largest aromatic ring system that can be accommodated in the nanocages of the catalyst. The mass transport of reactants and products will be greatly reduced with the accommodation of these bulky coke species, which cause the deactivation of the catalyst.[4] Considering the quick deactivation of SAPO-34, the fluidized-bed is applied in the industrial MTO process with reaction-regeneration cycle to keep the activity of catalyst.[63]

Table 1. Reaction Results of Methanol, Ethene, and Co-Feeding of Both over ZSM-22[66]

run no.[a,b]	1			2		3		
feed/ml per min								
CH_3OH	20			0		20		
C_2H_4	0			40		40		
He	40			20		0		
TOS/min	6	60	87	6	25	6	33	60
outlet/C-mol %								
C_2H_4	12.3	0.23	0.22	98.7	98.8	61.8	73.8	77.5
C_3H_6	29.0	0.10	0.06	0.11	0.09	14.1	5.62	2.35
C_4^+	51.1	0.37	0.13	1.18	1.08	17.6	3.94	0.37
CH_3OH/CH_3OCH_3	3.47	98.5	99.2	-	-	6.11	16.5	19.7
C_1^0-C_3^0	4.13	0.80	0.42	0.04	0.03	0.31	0.16	0.11
CH_3OH conv. %[c]	96.5	1.51	0.83	-	-	71.0	21.7	6.60
C_2H_4 conv. %	-	-	-	1.33	1.21	21.6	6.51	1.78
C_3H_6 sel. C-mol %	30.0	6.80	6.64	8.15	7.47	44.0	57.8	83.0

[a]T = 500 °C, ethene WHSV = 18 h^{-1}, methanol WHSV = 10 h^{-1}. [b]Three reaction runs were successively carried out without changing the catalyst sample. In the first run, only methanol was fed. Then the catalyst bed was purged with helium and only ethene was fed (run 2). After the following helium flushing, the coreaction of ethene and methanol was conducted (run 3). [c]Conversion was calculated with CH_3OCH_3 included.

In the R&D history of DMTO technology, in parallel to the process development, the methanol conversion mechanism was also studied in order to enhance catalyst performance, optimize the reaction conditions, and develop new highly selective catalysts.

3.1. Methylation in MTO Reaction. Our study on coreaction of ethene and methanol over different zeolites, SAPO-34, ZSM-22, ZSM-5[64−68] shows that there are at least three types of reactions involved in the coreaction system: the direct conversion of methanol (MTO), the direct conversion of ethene, and the methylation of ethene by methanol. The competitions among the three types of reactions are strongly influenced by the catalyst acid properties and can also be altered by catalyst modification. Complete suppression of direct conversion of methanol or ethene can be achieved over ZSM-22 and modified ZSM-5.[66,67] Using precoked ZSM-22 catalyst, on which the conversion of sole methanol or sole ethene is very low, cofeeding methanol and ethene gives rise to enhanced methanol conversion and ethene conversion, and at the same time, propene selectivity attains to higher than 80% at prolonged reaction time (Table 1).[66] Over hydrothermally treated P, La modified ZSM-5 catalysts with extremely weak acidity, ^{12}C-ethene and ^{13}C-methanol are co-fed and the isotopic distribution of propene indicates that most propene (89%) contains one ^{13}C atom from methanol, implying ethene methylation by methanol is responsible for the enhancement of conversion and propene generation in the coreaction system.[64] The further methylation of propene generates butane-2 with 2 ^{13}C atoms from methanol.[64] We also observe the same trend over SAPO-34, on which propene selectivity is also improved in the co-feeding system.[65,66] These results indicate that over the modified catalyst with weak acidity, the HCP mechanism cannot work, and therefore, alkene methylation and the cracking route will become the efficient and selective route for olefin production. In the normal MTO process with high methanol conversion, the methylation reaction should always be present, but it is implicit in the reaction system. This interesting methylation reaction could be useful for higher olefin production, such as the production of propene from the coreaction of ethene and methanol, and for adjusting the ethene/propene ratio in the MTO reaction.

3.2. Observation of Important Carbenium Ions and Their Role in Olefin Generation. Heptamethylbenzenium cation (HeptaMB$^+$) is of particular importance as a reaction intermediate in the MTO reaction,[4,69] and its synthesis has been made by the coreaction of benzene and methanol over H-beta, H-MCM-22, and H-mordenite.[8,9,50] However, over the molecular sieves with narrow eight-membered ring pore opening such as SAPO-34, the coreaction of benzene and methanol is unfeasible because of the diffusion limitations. A breakthrough of HeptaMB$^+$ observation was made by use of a newly synthesized catalyst DNL-6,[70−72] a eight-membered ring SAPO molecular sieve with an RHO structure possessing large α cages and relatively high acid concentration and strength, which can accommodate and stabilize the bulky carbenium cations. For the first time, heptaMB$^+$ is directly captured over DNL-6 by solid-state NMR during methanol conversion under real working conditions (Figure 1), and this observation is
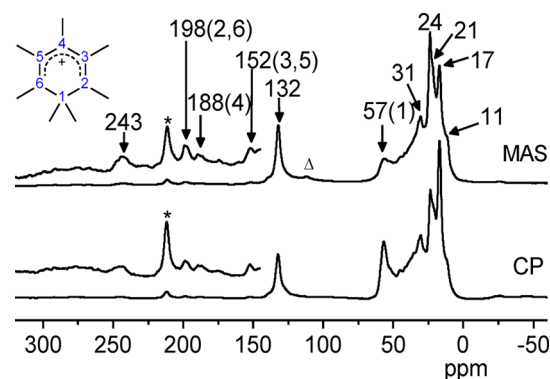

Figure 1. ^{13}C MAS and CP/MAS NMR spectra of the DNL-6 catalyst after ^{13}C-methanol conversion at 275 °C for ~50 min. * indicates the spinning sideband and Δ indicates the background.[73]

consolidated by GC−MS measurement of confined organics in the catalyst.[64,65] The ^{12}C/^{13}C-methanol switch experiments confirm the higher reactivity of polymethylbenzene than that of methylbenzenes with less methyl group substitution, implying the important role of these intermediates in the olefin formation.[73,74]
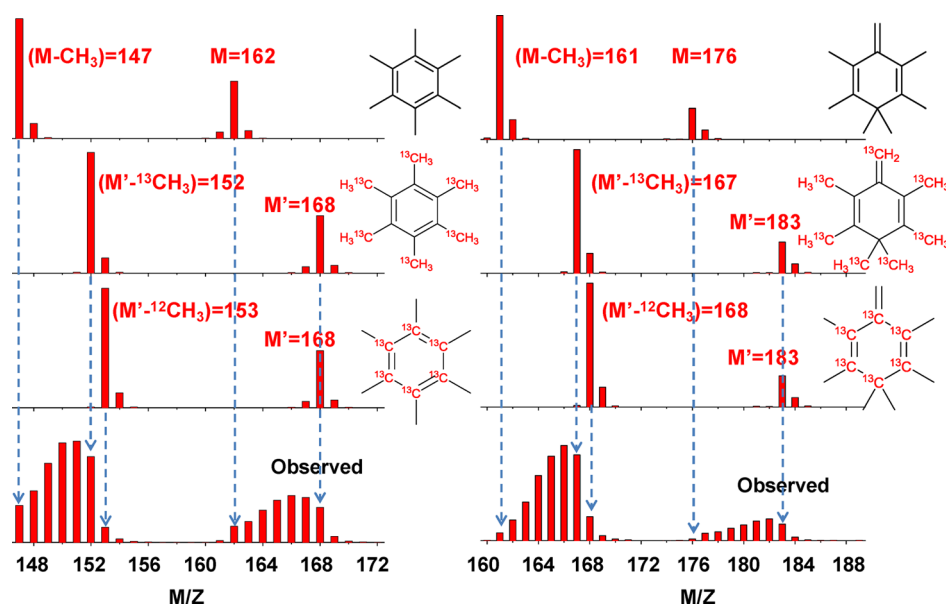
Figure 2. Comparison of mass spectra of hexamethylbenzene (left) and HMMC (right) obtained in the isotopic switch experiments over DNL-6 (9 μL of ^{13}C-methanol injection after continuous flow ^{12}C-methanol conversion for 60 min at 275 °C, WHSV of MeOH = 2.0 h^{-1}, He/MeOH (in mol) = 3) with the mass spectra of ^{12}C-HMB and HMMC (M) and simulated mass spectra of ^{13}C- labeled HMB and HMMC (M′).[73]

The difference of paring and side-chain methylation mechanism is whether the reaction route involves the ring contraction of benzenium cations and the ring expansion of cyclopentenyl cations or not. The isotopic switch experiments offer the evidence for the suggested reaction route (Figure 2).[73] In the mass spectra of hexamethylbenzene (HMB) and hexamethylmethylenecyclohexadiene (HMMC, the deprotonated form of heptaMB$^+$), one notable observation is that the number of ^{13}C atoms incorporated into HMB or HMMC is less than that of the substituted methyl groups (6 or 7). The most incorporated ^{13}C atoms are exactly the total count of methyl groups in the molecules. The other notable observation is that the M/Z gap between molecular ions of HMB (or HMMC) and the molecular ions with one methyl group lost is 16, indicating the location of all six ^{13}C atoms of hexamethylbenzene (or seven ^{13}C atoms of HMMC) in the methyl groups rather than in the benzene ring. These two observations prove the feasibility of methanol conversion via side-chain methylation mechanism, which involves a key step of methylation of hexaMB to form heptaMB$^+$ for further methylation and elimination to generate olefin products. (Figure 3).[74]

We also succeed in observing the simultaneous formation of heptamethylbenzenium cation (heptaMB$^+$) and pentamethyl-cyclopentenyl cation (pentaMCP$^+$) under the real working conditions of methanol conversion over the catalyst with CHA topology,[75] which made it possible to elucidate the reaction mechanism over the industrial DMTO catalyst. The observations of heptaMB$^+$ and pentaMCP$^+$ and the correlation between their concentration and methanol conversion mean that both of the two reaction routes, i.e., the paring route and side-chain methylation route, are possible for methanol conversion over the catalyst with CHA topology. The theoretical calculation predicted the reaction pathway with the involvement of heptaMB$^+$ and pentaMCP$^+$ as the intermediates. Both of the two reaction routes for propene production are energetically feasible, while the side-chain methylation mechanism is predominant due to the lower energy barrier.
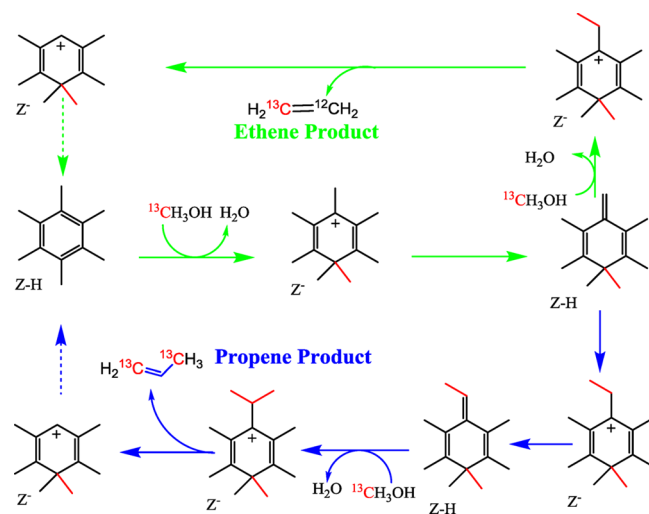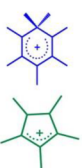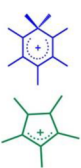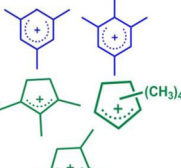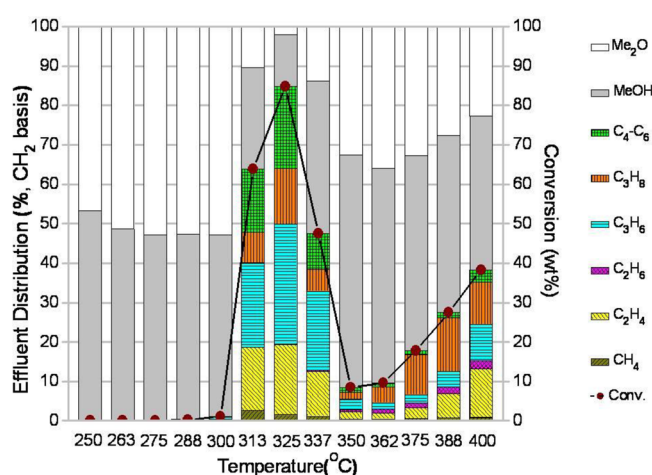

Figure 3. Side-chain methylation mechanism for olefin generation over DNL-6.[74]

Using the techniques including in situ ^{13}C NMR and GC-MS, we systematically investigated the confined intermediates in SAPOs and other zeolites with the same eight-membered ring and different supercages.[76,77] The results are summarized in Table 2. These results indicate that the HCP mechanism is generally effective for the reaction; however, the carbenium cations vary with the cavity size with some extent of diversity. In smaller cages, the cations are formed with less substituted methyl group or smaller molecular size. Although shape-selectivity is commonly believed to be effective for these eight-membered ring molecular sieves in the MTO reaction, cavity still has great influence on selectivity considering the big difference of their product distributions. It seems that cavity controls the selectivity if the ring-opening of molecular sieves has the same size.[77]

3.3. Deactivation at Low Reaction Temperature. An interesting phenomenon, as shown in Figure 4, is observed

Table 2. Carbenium Ions Observation in Cage-Type Eight-Membered Ring Zeolite Catalysts

Cage type	RHO	CHA	LEV
Cage size (nm)	1.14×1.14	0.67×1.00	0.63×0.73
Materials	DNL-6	SAPO-34	SAPO-35
		H-SSZ-13	H-RUB-50
Carbenium ions			

Figure 4. Effluent distribution of fluidized-bed methanol conversion under the condition of programmed increase of temperature.

when we study the temperature-programmed methanol conversion in a microscale fluidized-bed reactor.[78] When the reaction is fed at 250 °C, no methanol conversion occurs. Only methanol and dimethyl ether appear in the effluents until the

temperature gradually increases to 300 °C, showing an obvious induction period of methanol reaction. At the temperature range of 300−325 °C, light olefins and other hydrocarbons appear among the effluents, and the yield of hydrocarbon products increases with temperature. It is worthy to note the particular and remarkable decline of methanol conversion in the following period with temperature increase from 325 to 350 °C. When the temperature is further increased to 400 °C, the catalyst reactivity is partially recovered, and methanol conversion is improved again during this period. This particular observation drives us to study the catalyst deactivation of methanol conversion at low temperature.

Isothermal methanol conversion carried out at low reaction temperature (300−350 °C) under the same condition presents an obvious induction period and quick deactivation.[79,80] The induction period is shortened with an increase in reaction temperature. Diamondoid hydrocarbons largely form and are retained in the SAPO-34 catalyst as a kind of newly found residue hydrocarbon. Different from polymethylbenzenes, the reaction center of the MTO, ^{12}C/^{13}C methanol switch experiment performed over the catalyst with confined polymethylbenzene and polymethyladamantanes confirms that the confined methyladamantane molecules are inactive when contacting with the feed of methanol. The accumulation of these cyclic and saturated hydrocarbons in the catalyst blocks the access of methanol to methylbenzenes and suppresses the successive generation of the HCP species, accounting for the quick deactivation of SAPO-34 at 300 °C (Figure 5).[79] On the basis of this study carried out at low temperature under isothermal condition, we combine the confined coke species evolution with the catalytic performance of methanol reaction under the condition of temperature-programmed increase. In the temperature range of 300−350 °C, beside the formation of methylbenzenes as the active reaction center, methyladamantanes are largely formed and cause the occurrence of deactivation at the temperature range of 325−350 °C. With the temperature increase, methylbenzenes and methyladamantanes are transformed to methylnaphthalenes and polycyclic aromatics at higher temperature. The evolution of the confined organics corresponds to the initial reactivity enhancement of the catalyst at temperature range of 300−325 °C, the lowered reactivity at 325−350 °C, and recovered methanol conversion at 350−400 °C (Figure 4).[78] Some extended work indicates
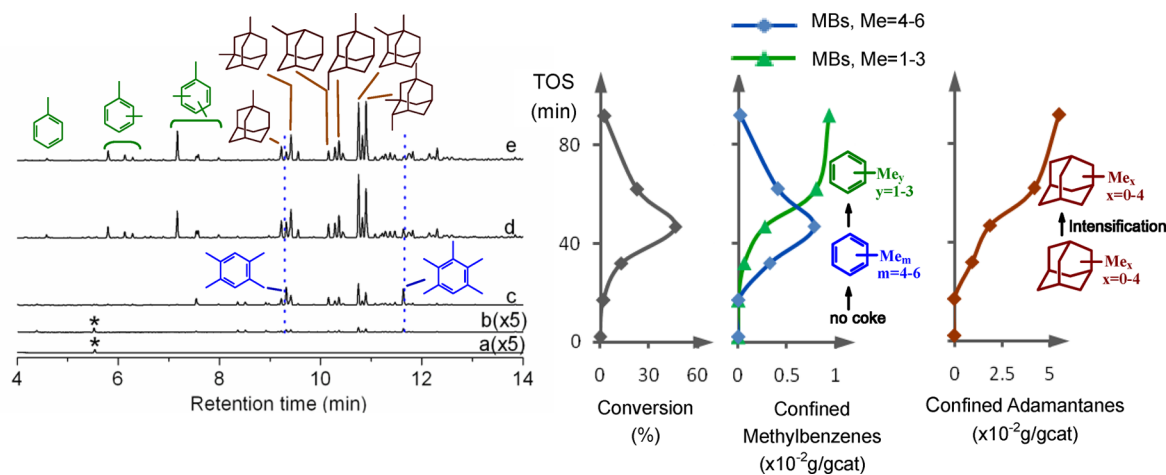
Figure 5. GC-MS analyses (left) of confined organics after methanol conversion at 300 °C for 17 (a), 32 (b), 47 (c), 62 (d), and 92 min (e); Methanol conversion (middle) and methylbenzenes and methyladamantanes (right) variation with time on stream. * internal standard.[79]

adamantane hydrocarbons can also be formed and accommodated in other eight-membered ring and cage-type SAPO molecular sieves with AEI and LEV topology. These cage type molecular sieves provide the catalytic surrounding for the formation of adamantane hydrocarbons as confined products in methanol conversion under the reaction condition of low temperature.

During methanol conversion, coke deposition over the catalyst has been also studied with TEOM (tapered element oscillation microbalance) under the real reaction condition.[80,81] The coking rate is quite different at various reaction temperature. High- (500 °C) and low-temperature (300 °C) reactions present higher coking rate than the reactions performed under mild reaction condition (400−450 °C).[80] The extremely high coking rate at low reaction temperature corresponds to the quick deactivation during methanol conversion with predominant adamantane hydrocarbons formation and accommodation in the catalyst.

3.4. Reaction Network. Our studies of methanol conversion over zeolites and SAPO catalysts with different topology indicate that the aromatics-based HCP reaction mechanism is dominant for the MTO reaction over SAPO-34 than on ZSM-5 and ZSM-22.[65−68] Dual-cycle reactions proceed over ZSM-5 catalyst, and olefins methylation and cracking mechanism occurs in the reaction over ZSM-22.[66−68] Even the significant contribution of the HCP mechanism for cage-type SAPO catalysts, olefin methylation and cracking mechanism also works in some cases. The acid density variation plays different roles in the alkenes-based cycle and aromatics-based cycle. When methanol conversion to light olefins takes place over the eight-membered ring AlPO-18 and SAPO-18 with AEI cavity, the catalyst with high-density Brønsted acid sites can accelerate the formation and accumulation of cyclic organic species over the catalysts. The aromatics-based HCP mechanism plays an important role for methanol conversion over SAPO-18 with more Brønsted acid sites; however, over AlPO-18, because the carbenium ions cannot be formed over nonacidic catalyst, the conversion is very low and, the formation of olefins mainly follows olefin methylation and cracking route.[82]

In the actual methanol reaction over acid zeolites or SAPO catalysts, considering the occurrence of all the possible competitive reactions, including the olefin formation reaction through aromatics-based or olefins-based reaction route (i.e., olefin methylation, olefin oligomerization, and cyclization, olefin cracking, and other reactions which may cause deactivation), a reaction network is proposed and presents a complicated reaction system (Figure 6), in which some reactants and products are reciprocal or overlapped in a series of reactions following different reaction routes. There are two main reaction modes in the network related to coke formation, one by further transformation of HCP intermediates and the other one by further conversion of olefin products without
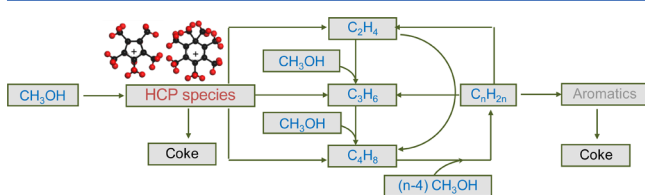
involving HCP intermediates. In principle, the first coking reaction can be restricted by selecting molecular sieve catalyst with suitable cavity size, which could be a possible way to enhance the catalyst lifetime.

4. SYNTHESIS AND CRYSTALLIZATION MECHANISM OF SAPO MOLECULAR SIEVES

Silicoaluminophosphate (SAPO) molecular sieves were first invented by the scientists at Union Carbide Corporation in 1984.[83,84] Among the SAPOs, SAPO-34 with the CHA structure is particularly interesting and demonstrates excellent catalytic performance in the MTO reaction due to the contribution of small pore, medium acidity, and high thermal/hydrothermal stability.[15,21,85,86] The CHA framework topology, characterized by cylinder-like cages with eight-membered ring openings, has been evidenced to be the ideal breeding ground for hydrocarbon pool intermediates in the MTO reaction.[36,48]

Hitherto, many research works have been reported on the synthesis, physicochemical and catalytic properties of SAPO-34.[87−100] DICP has also dedicated great efforts to the synthesis and crystallization mechanism of SAPO-34, as well as the relationship among the Si coordination environment (acidity), Si distribution, and the MTO catalytic performance. In the late 1980s, DICP first reported the excellent catalytic performance of SAPO-34 in the MTO reaction and its good regeneration stability.[85,101] This exciting finding was further strengthened by our following investigations on the hydrothermal stability of SAPO-34, which kept more than 80% relative crystallinity after 100% steam treatment at 800 °C for 45 h.[102] These results confirmed that SAPO-34 could be taken as a promising MTO catalyst for industrial application. In the subsequent researches, much attention was paid to explore new templates for the SAPO-34 synthesis, considering that templates may influence the morphologies, microstructures, and acidic properties, and thus lead to optimized catalytic properties. We found that, as an example, triethylamine (TEA), diethylamine (DEA), and their mixtures could direct the crystallization of SAPO-34 with good catalytic results.[103−105] The observations were attractive from the practical perspective because these amines were much cheaper than the traditional tetraethylammonium hydroxide (TEAOH), and their use would greatly reduce the cost for manufacture of the catalyst. Subsequently, a symmetric investigation on the relationship of syntheses, Si coordination environments, and catalytic properties were carried out.[106−109] It was recognized that SAPO-34 with lower Si content, corresponding to the major existence of Si(4Al) species in the framework (medium/strong acidity), generally had higher olefins' selectivity and longer lifetime. As shown in Figure 7, with the rising of Si content in the SAPO-34, the Si coordination environments become complex, and the corresponding acid strength/concentration increases. SAPO-34(a) catalyst with low Si content and single Si(4Al) species exhibit long lifetime and low hydrogen transfer index (corresponding to the low selectivity of propane and slow coking rate). Further studies then focused on the crystallization process of SAPO molecular sieves to understand the mechanisms governing the nucleation, crystallization, and Si distribution for a better control of composition and Si environmental of the synthetic product.[110−113] The insight on the crystallization mechanisms has been proved to be an effective way to optimize the synthesis of SAPO-34 with improved catalytic properties.


Figure 6. Reaction network of methanol conversion.
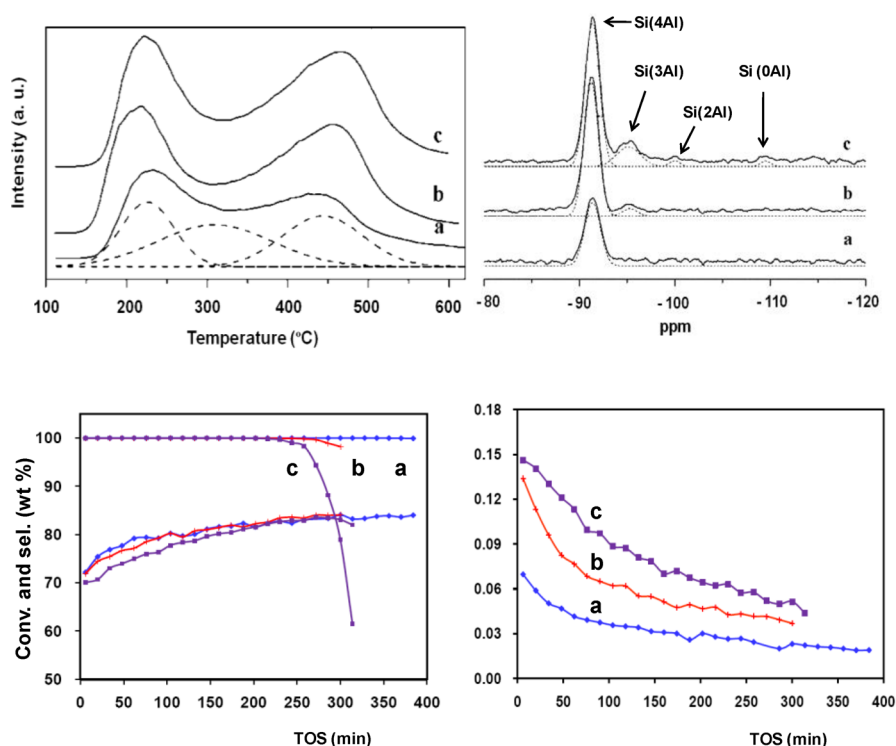
Figure 7. NH$_3$-TPD profiles (top-left) and ^{29}Si MAS NMR spectra (top-right) of SAPO-34s and their MTO catalytic results (bottom-left). SAPO-34 was synthesized with TEA template (3TEA:1Al$_2$O$_3$:1P$_2$O$_5$:xSiO$_2$:50H$_2$O, 200 °C, 48 h). a: x = 0.2; b: x = 0.4; c: x = 0.6. Reaction conditions: T = 450 °C, WHSV = 1.2 h^{-1}, 30 wt % methanol solution. Hydrogen transfer index (HTI) over the catalysts is shown in the bottom-right of the figure.

In the early research stage, when the understanding of molecular sieves was relatively poor, it was difficult to determine which molecular sieve could best fit the specified application because many small-pore SAPO molecular sieves, such as SAPO-44, -17, -18, -35, -56, and so forth, could be potentially used as shape-selective catalysts as far as the pore size openings are concerned. We synthesized all SAPOs mentioned above and explored their MTO performances.[114,115] Unfortunately, all of them exhibited inferior catalytic performance (both the lifetime and selectivity to ethene plus propene) to SAPO-34. Furthermore, various MeAPSOs and metal-modified SAPO molecular sieves including SAPO-34 were also investigated, and some of them showed obvious improvement in the selectivity to olefins.[114,116,117] However, in most cases, the increasing amount of CO and CO$_2$ could be found in the reaction product due to the existence of transitional metals that may cause the decomposition of methanol.

4.1. CRYSTALLIZATION MECHANISM AND SI DISTRIBUTION IN THE CRYSTALS

Crystallization mechanism is an interesting issue in the study of molecular sieves, which can offer a more rational approach to the design and synthesis of molecular sieves with optimized acidic/catalytic properties.

Crystallization of SAPO-34 was first studied with TEA template at 200 °C from a gel composition of 3TEA:0.6-SiO$_2$:Al$_2$O$_3$:0.8P$_2$O$_5$:50H$_2$O.[110] Figure 8 illustrates the proposed model of SAPO-34 crystallization and the Si incorporation mechanism. It is found that preliminary structure units similar to the framework of SAPO-34 have already formed before the crystallization start (0 h and low temperature), and the nucleation of SAPO-34 comes from the structure rearrangement of the initial gel and the condensation of the
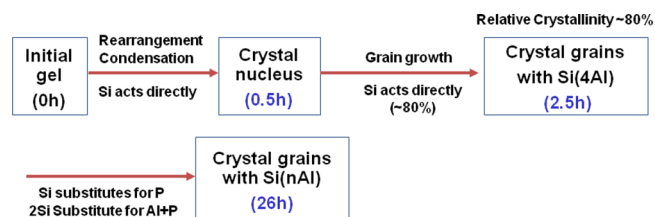
Figure 8. Model of the SAPO-34 crystallization process and the Si incorporation mechanism.[110]

hydroxyls. The solution support is important for further crystallization of SAPO-34. Regarding the Si incorporation, it reveals that Si atoms directly take part in the formation of the crystals. At the early stage of the crystallization (<2.5 h), a SM2 mechanism occurs (substitution of P by Si), generating a Si(4Al) environment. Subsequently, the relative content of Si in the products increased slowly, and Si environments become complex (Si(nAl), n = 0−4), suggesting the co-occurrence of SM2 and SM3 (substitution of P−Al pair by 2Si) mechanisms.

Further investigation on the crystallization of SAPO-34 templated by DEA (2DEA:0.6SiO$_2$:Al$_2$O$_3$:0.8P$_2$O$_5$:50H$_2$O, 200 °C) gives similar conclusion as that by TEA system about the crystal formation/growth and Si incorporation mechanism.[118] Higher Si incorporation amount into the framework was observed with DEA template, possibly due to the smaller molecule size of DEA. This is also consistent with the higher DEA molecular density in the CHA cage (1.75 DEA vs 1.0 TEA per cage). Notably, a nonuniform distribution of Si atoms in the crystals was revealed, which shows a gradual increase from the core to the surface (Figure 9). Given that the acid strength corresponding to different Si species in SAPO molecular sieves has the order of Si(1Al) > Si(2Al) > Si(3Al) > Si(4Al),[119] this
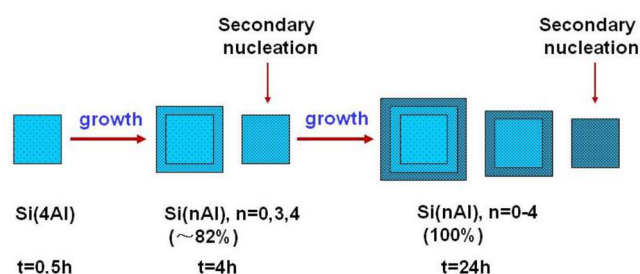
Figure 9. Schematic diagram of the crystallization process of SAPO-34 with Si distribution in the crystals. The dot density in the square stands for the Si concentration in the crystals.

finding suggests that the acidic sites along the crystals are not uniformly distributed and the stronger acidic sites are more likely concentrated on the external surface. As shape-selective reaction always causes diffusion effect, it is reasonable to speculate that the stronger acidic sites on the external surface would have high priority for the reaction and cause less selectivity and more coke formation.[120] The larger coke compounds formed in the cages at the edges of the crystals may further cause diffusion limitation and inhibit the release of product generated inside. It implies that the surface Si enrichment phenomenon is detrimental to the MTO reaction, which should be avoided for a better shape selectivity of the MTO reaction.

Besides SAPO-34, three other SAPO molecular sieves (SAPO-35, -11, and -5)[111,112] with different topological structures were also investigated with respect to their hydrothermal crystallization process, in order to gain a comprehensive understanding of the synthesis mechanisms. Although the concrete crystallization process of each SAPO molecular sieve is different from others, there are still some common features that could be concluded as follows: (1) the crystal growth follows a solution-mediated transport mechanism; (2) Si atoms incorporate into the SAPO frameworks from very beginning of the crystallization and their content in the products increase gradually; (3) the silica enrichment on the crystal surface occurs for all SAPO samples investigated (Table 3), and the extent is influenced by the framework type and synthetic conditions.

Table 3. Bulk and Surface Compositions of SAPO Molecular Sieves

sample[a]	elemental composition (mol %)		$Si_{surface}/Si_{bulk}$
	XRF	XPS	
SAPO-34-T	$Si_{0.080}Al_{0.486}P_{0.434}$	$Si_{0.206}Al_{0.453}P_{0.341}$	2.58
SAPO-34-D	$Si_{0.164}Al_{0.478}P_{0.358}$	$Si_{0.231}Al_{0.440}P_{0.329}$	1.41
SAPO-5	$Si_{0.073}Al_{0.488}P_{0.439}$	$Si_{0.155}Al_{0.420}P_{0.424}$	2.12
SAPO-11	$Si_{0.045}Al_{0.498}P_{0.458}$	$Si_{0.224}Al_{0.462}P_{0.314}$	4.98
SAPO-35	$Si_{0.122}Al_{0.488}P_{0.390}$	$Si_{0.187}Al_{0.478}P_{0.335}$	1.53

[a]Data from ref 111. SAPO-34-T and SAPO-34-D were synthesized with TEA and DEA as the template, respectively.

4.2. Synthesis of SAPO-34 with Single Si(4Al) Environment.

One simple way to control the Si coordination environment in SAPO-34 is to vary the Si content in the starting gel. However, the synthesis of SAPO-34 with only the Si(4Al) environment is difficult because crystal impurities may form together with SAPO-34 when employing low Si content. Crystallization conditions and starting materials should be

carefully controlled to achieve a successful synthesis.[118,121,122] According to our crystallization research, the initial gel with medium/high Si content and shortened crystallization time would also provide an easy approach to produce SAPO-34 with single Si(4Al) species, which, however has a low product yield.

Fluorine-mediated synthesis has been widely employed in zeolite crystallization due to the effective mineralization ability of F^- ions. It can form chelates with the reaction sources (Al/P/Si) and promote the dissolution of pseudoboehmite and silica particles. With the assistance of fluoride, crystals with fewer framework defects could be obtained. Table 4 displays

Table 4. MTO Reaction Results over SAPO-34 Synthesized with and without HF[a]

| sample		SAPO-34	SAPO-34-F
product composition		$Si_{0.10}Al_{0.49}P_{0.41}$	$Si_{0.09}Al_{0.50}P_{0.41}$
Si(4Al)/Si(3Al)[b]		2.75	66.35
lifetime (min)[c]		120−140	180−200
selectivity (wt %)	CH_4	0.93	0.89
	C_2H_4	31.29	35.66
	C_2H_6	0.84	0.69
	C_3H_6	39.55	38.41
	C_3H_8	7.04	5.03
	C_4	11.66	10.83
	C_5^+	8.69	8.49
	$C_2^=+C_3^=$	70.84	74.07

[a]Reaction conditions: T = 450 °C, WHSV = $2h^{-1}$, N_2 as carrier gas, TOS = 20 min. Gel compositions for the synthesis are $3TEA:1Al_2O_3:1P_2O_5:0.6SiO_2:xHF:50H_2O$ (200 °C, 12h). x = 0 and 0.33 for SAPO-34 and SAPO-34-F respectively; [b]Determined from ^{29}Si MAS NMR spectra; [c]Reaction duration with 100% methanol conversion.

the product compositions, Si(4Al)/Si(3Al) ratios, and MTO results of SAPO-34-F (HF/Al_2O_3 = 0.33 in the initial gel) and conventional SAPO-34.[123] Dominant Si(4Al) species appear in the SAPO-34-F sample, giving longer lifetime and lower alkane selectivity, although the two samples show similar product compositions. Given that SAPO-34-F possesses similar textural properties to conventional SAPO-34, it is reasonable to attribute the improved catalytic performance of SAPO-34-F to its optimized Si coordination environments and further to the corresponding acidity. Moreover, it is speculated that the formation of fluoride-Si chelates would lead to a relatively homogeneous release of Si during the crystallization and thus reduce Si enrichment on the external surface of SAPO-34 crystals, as compared to the case without fluoride.

In an attempt to lighten the Si enrichment on the external surface, a facile postsynthesis modification method was developed by treating as-synthesized SAPO-34 with HF or NH_4F solution.[107] As shown in Figure 10, both the relative crystallinity and Si content of the sample decrease following the increasing HF concentration. In the meantime, the external surface of SAPO-34 becomes rather rough, and Si species other than Si(4Al) gradually diminish. This implies that F^- ions selectively remove Si atoms in the Si-rich regions of the crystal surface. All modified samples exhibit prolonged lifetime with a maximum over SAPO-34−0.1HF sample (0.1 mol/L HF solution used for the post-treatment).

4.3. Novel Methods To Synthesize SAPO-34.
A solvothermal synthesis route designated as aminothermal synthesis, in which organic amines are used as both the
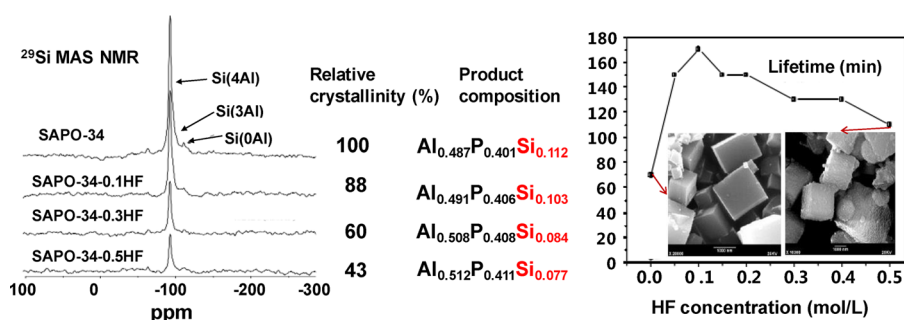
Figure 10. ^{29}Si MAS NMR spectra, relative crystallinity, product compositions, and MTO reaction lifetime of SAPO-34 before and after treatment with HF solution (RT, 12h). Reaction conditions: T = 450 °C, WHSV = 2h^{-1}, N$_2$ as carrier gas.

dispersing medium and the template, has been developed for the synthesis of SAPO-34.[124−126] The main features associated with this method are the high solid yield and fast crystallization rate, which is important from the practical perspective. For example, 90% and 96.2% yields are acquired after 12 h at 200 °C on the basis of *N,N,N′,N′*-tetramethylethylenediamine (TMEDA) and di-iso-propylamine (DIPA) systems, respectively. The less solubility of inorganic resources in the aminothermal system should be the main reason for the increased solid product yield. Investigation on the amino-thermal crystallization process revealed that at first a lamellar AlPO material is formed, which promotes the dissolution of resources and leads to a faster crystallization rate. Significantly, SAPO-34 templated by DIPA shows good MTO catalytic performance with an ethene plus propene selectivity of 85.8%. Further extending this method to other amine systems, several novel templates for the synthesis of SAPO-34 have been discovered, such as diisopropanolamine, diglycolamine, and *N*-methyldiethanolamine. Moreover, a phase-transformation method has been proposed to synthesize SAPO-34 by using other SAPO molecular sieves as precursors.[72] This approach provides a possibility to transform crystals containing SAPO impurities to pure SAPO-34 product.

The synthesis of nanosized or hierarchical SAPO-34 has attracted great attention because it can reduce the diffusive limitation and lead to an improved MTO catalytic lifetime. Many strategies have been reported, and most of them involve the use of expensive TEAOH as the template.[13,127−132] A top-down route (postsynthesis, milling, and recrystallization) has been developed to prepare SAPO-34 nanocrystals by using TEA template.[133] The obtained nano-SAPO-34 shows considerably improved catalytic performance (Figure 11), resulting from a combination of shortened diffusion paths, decreased acid concentration, and reduced Si enrichment on the crystal surface. This method is further proven to be generally applicable to prepare other SAPO nanocrystals. Furthermore, hierarchical SAPO-34 has also been synthesized using organosilane surfactant as part of silica source and mesoporogen with TEA or DEA as a micropore template.[134]

5. CATALYST AND SCALE-UP

5.1. Scale-Up Synthesis of SAPO-34. DICP first scaled up the synthesis process of SAPO-34 in 1993 by employing a 1 M^3 autoclave, aimed to supply catalyst (named as DO123) for the pilot-scale SDTO test. In 2005, a pilot catalyst synthesis plant with two 2 M^3 autoclaves, which was close to a commercial scale to some extent, was built up. The purposes of the scale-up of the syntheses process were as follows: (1) to
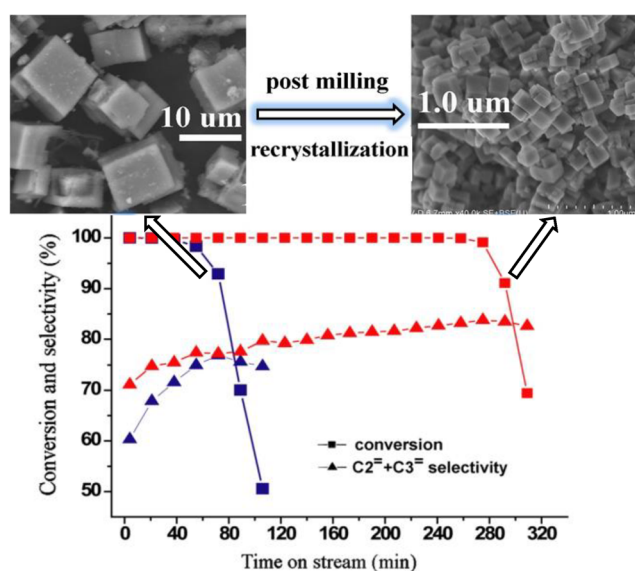

Figure 11. SEM images and MTO results of SAPO-34 before and after postsynthesis milling and recrystallization. Reaction conditions: T = 450 °C, WHSV = 4 h^{-1}, 40% methanol solution.[133]

supply molecular sieve for the production of DMTO catalyst used for the demonstration unit; (2) to verify the reproducibility and reliability of the synthesis technology; (3) to find and solve problems that may exist in the large scale catalyst manufacture such as heating rate, mixing homogeneity (stirring), and solid−liquid separation; (4) to further optimize the synthetic conditions and reduce cost; (5) to establish an entire catalyst quality control system for the synthesis process. On the basis of the data and experiences from the pilot synthesis plant, the industrial production of SAPO-34 in a large scale was realized in 2008.

5.1.1. Synthesis Planning. The choice of a synthesis procedure suitable for industrial catalyst manufacture should consider many factors. Good catalytic performance in MTO reaction is of particular importance. Meanwhile, solid yield, crystallization rate, and operational feasibility should also be taken into account. The synthesis of SAPO-34 developed by DICP employs TEA, DEA as the templates. The product has the characteristics of rapid crystallization, adjustable acidity, and particle size. More importantly, the present template has a lower boiling point (below 100 °C) than water. After the synthesis, the amine could be easily separated from the mother liquid through flash distillation and reused for the synthesis, which could reduce the cost for synthesis and the following waste treatment. It is worth noting that all raw materials used in

the synthesis scale-up are commercially available, and only those who could provide a long-term supply with steady quality can be selected as the suppliers.

5.1.2. Process of the SAPO-34 Scale-Up Synthesis. The process flow diagram of the synthesis is shown in Figure 12.
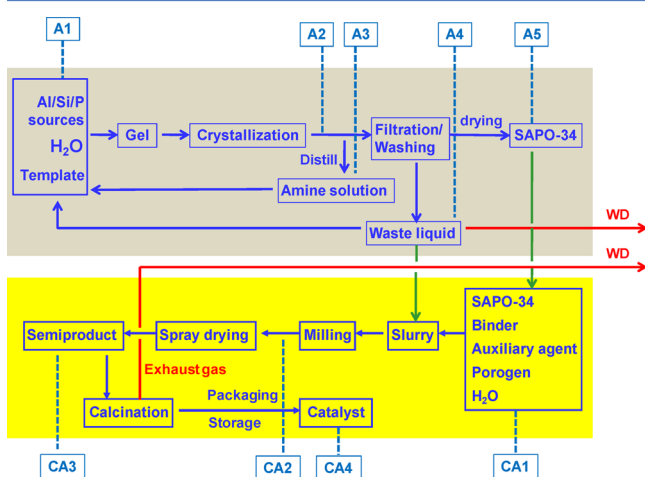
Figure 12. Process flow diagrams of the SAPO-34 synthesis (top) and catalyst preparation (bottom). The quality control points of each process have been labeled in the diagrams as A1−A5 and CA1−CA4. WD refers to waste disposal.

The synthetic procedure is as follows: the Si/Al/P/template resources were mixed with deionized water according to a predetermined sequence and stirred to achieve a homogeneous gel. The autoclave is then sealed and heated to the crystallization temperature. After the crystallization is complete, the autoclave is quenched by cooling medium to 90 °C, a temperature at which the residue of organic amine was distilled out and collected. When the autoclave is further cooled to below 50 °C, solid products can be recovered by filtration, washing with deionized water, and drying in the air.

The recovery of amine during the cooling period is important from the economic and ecological viewpoints, which could improve the environment of subsequent filtration unit and reduce the liquid waste disposal. After GC-MS analysis of the collected amine solution, it can be readily recycled for the synthesis. The obtained SAPO-34 shows good crystallinity and catalytic performance, which is almost identical to the product synthesized with fresh amine. Moreover, a large amount of waste liquid generated from the synthesis (filtration/washing), containing unreacted chemicals, can also be reused after analyzing the solid content. The synthesis with recycled liquid has rapid crystallization rate and higher solid yield. This is likely due to the small amount of crystals/nuclei (seeds) in the recycled liquid. These approaches reduce the emission of waste and the cost of synthetic process, and make the process more environmental friendly.

5.1.3. Quality Control of SAPO-34 Synthesis. Establishment of the quality control system and standard test method/procedure for the synthesis process is also important to keep the product quality and maintain a steady production. Figure 12 illustrates the quality control points of the SAPO-34 synthesis process (A1−A5). A1 is about the analyses of incoming raw materials to avoid the use of unqualified materials. A2 measures the crystal phase and purity of the solid in the synthesis slurry. A3 and A4 analyze the content of the distilled amine solution

and collected waste liquid, respectively, for their recycling use. A5 is the analyses of the SAPO-34 product including crystal phase, composition, morphology, textural properties, solid content, and catalytic performance. The qualified product would be delivered to the next unit for the microsphere catalyst preparation.

5.2. Catalyst Manufacturing Process Scale-Up. The DMTO catalyst with SAPO-34 as the active component is prepared by spray drying method and has the following characteristics: microsphere, particle size distribution similar to FCC catalyst, high mechanical strength (low attrition index), and good catalytic performance.[135−137] The manufacturing scale-up of DMTO catalyst was carried out in 2005, and ca. 25 tons of catalyst was successfully produced and supplied for the DMTO demonstration unit (16 kt/a MeOH feed). Subsequently, following the licensing of DMTO catalyst technology, a 2000 t/a DMTO catalyst plant (containing molecular sieve synthesis and catalyst manufacturing) was constructed and put into production in 2008.

5.2.1. Process Flow of the Catalyst Manufacturing. The process flow diagram of the catalyst manufacturing is illustrated in Figure 12. The manufacturing procedure is as follows: SAPO-34, binder, auxiliary agent, porogen, and deionized water are mixed under stirring and milled to achieve sufficient uniform slurry. The waste liquid generated in the synthesis section could substitute part of water for the catalyst manufacturing. The well-milled slurry is then fed to spray drier, by which microsphere catalyst is produced. Following a successive calcination, packaging, and storage, the final catalyst can be obtained.

5.2.2. Quality Control for Catalyst Manufacturing. The quality control points of the catalyst manufacturing process have been labeled in Figure 12 as CA1−CA4. CA1 is the analysis of the raw materials except the SAPO-34 molecular sieves. CA2 detects the particle size distribution of the milled slurry to ensure the effective dispersion/mixing of the components. CA3 measures the particle size distribution and morphology of the semiproduct, which provides feedback to the spray drying to keep the suitable particle size distribution for product. CA4 is the analysis of the calcined product, including the solid content, composition, morphology, particle size distribution, attrition index, textural properties, bulk density, and catalytic performance. Typical properties of the DMTO catalyst have been listed in Table 5. The typical morphology and particle size distribution is shown in Figure 13.

6. DMTO PROCESS DEVELOPMENTS

6.1. DMTO Reactor Selection. The MTO reaction over SAPO-34 catalyst is highly exothermic, and the heat of reaction is about −196 kcal/kg methanol feed when the reaction temperature is at 495 °C. The reaction heat must be removed from the reaction bed simultaneously to keep the reaction temperature in the designed range. In addition to that, the MTO reaction over SAPO-34 catalyst is featured by rapid catalyst deactivation due to the coke deposition. The methanol conversion shows a rapid drop after the coke amount on the catalyst reaching up to a maximum value (Figure 14). In order to maintain high activity of catalyst in the reactor, the in-line combustion of coke is required. At early stage, DICP had investigated the fixed bed reactor for MTO process. Subsequently, the fluidized bed reactor was considered superior to fixed bed reactor because of the excellent heat transfer performance and good fluidity of catalyst in fluidization state.

Table 5. Typical Properties of the DMTO Catalyst

BET surface area (m^2/g)		≥180
pore volume (cm^3/g)		≥0.15
attrition index (%/h)		≤2
density (g/cm^3)	bulk density	0.6~0.8
	dense packing density	0.7~0.9
	particle density	1.5~1.8
particle size distribution (%)^a	≤20 μm	≤5
	20~40 μm	≤10
	40~80 μm	30~50
	80~110 μm	10~30
	110~150 μm	10~30
	≥150 μm	≤20
catalytic performance^b	lifetime (min)	≥120
	optimal selectivity of C$_2$H$_4$ plus C$_3$H$_6$ (wt %)	≥86.5

^{a}Measured with laser particle sizer. ^{b}Test conditions: fixed-fluid bed, 10 g of catalyst, 450 °C, WHSV = 1.5 h^{-1}, 40 wt % methanol solution. The lifetime refers to the reaction duration of conversion >98% (methanol and dimethyl ether considered as reactant).
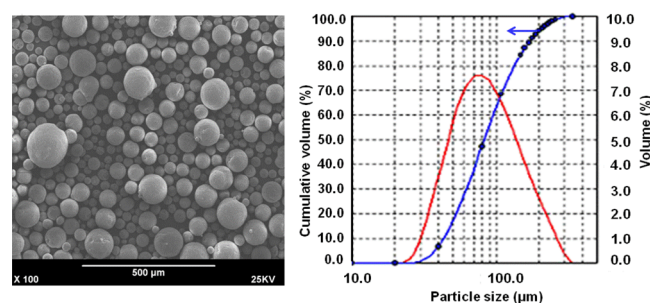

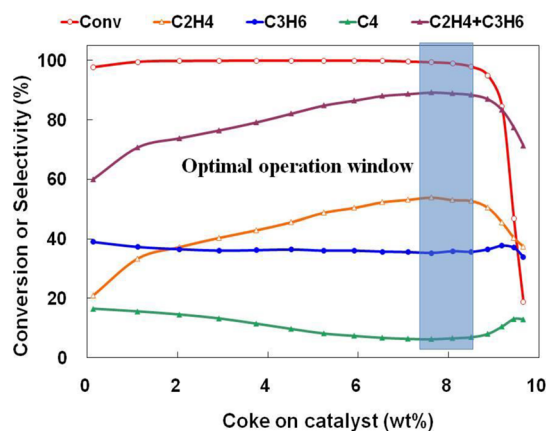**Figure 13.** SEM image and particle size distribution of DMTO catalyst.

Figure 14. Effect of coke deposition on the methanol conversion and selectivity to light olefins in microscale DMTO fluidized bed reactor at 450 °C.

On one hand, the great quantity of small catalyst particles can provide a very large surface area, and the heat transfer is rarely a problem in the fluidized bed. The temperature difference in the fluidized bed can be readily reduced to just several degrees via optimal operation. The heat removal is actually a common practice in fluidized bed processes in industries. One example is the catalyst coolers widely used in fluid catalytic cracking (FCC) units in modern refineries. On the other hand, the catalyst, when fluidized, can be transported between the reactor and regenerator like a liquid, which makes the continuous regeneration of catalyst in DMTO process possible. In the DMTO process, the fluidized bed reactor−regenerator configuration was adopted.

ExxonMobil and UOP have applied for many patents on the riser[18] and fast fluidized bed reactor[138] for the MTO process. In our early studies, different types of fluidized bed reactors were proposed and tested for DMTO process, which include two downer reactors and a dense phase fluidized bed reactor. It was found that the catalyst deposited with a certain amount of coke could favor the selectivity to ethene and propene even at high methanol conversion (>99%), as illustrated in Figure 14. An optimal operation window exists near the coke content of ∼8%. To achieve an average coke content of ∼8% in the reactor, catalyst residence time should be around 60 min subject to the reaction temperature and WHSV. In this connection, both the riser and downer reactors seem not suitable for DMTO process as the catalyst residence time is only several seconds, and the optimal operation window is hard to achieve without recycling the catalyst to accumulate coke on the catalyst. Furthermore, the methanol conversion is relatively low in either riser or downer reactor. In the DMTO process, the dense phase fluidized bed reactor is chosen.

Experiments in the laboratory showed that a catalyst−gas contact time of about 2−3 s is necessary in order to avoid undesired byproduct in the DMTO reaction. Such a short catalyst−gas contact time means that an industrial DMTO reactor has to be operated at a gas velocity higher than 1 m/s, which otherwise leads to a fluidized bed with bed height less than 3 m. This imposes a great challenge for engineering design as it is extremely difficult, if not impossible, to arrange gas distributor, cyclone diplegs, catalyst draw-off bin, and other internals in a space lower than 3 m. Actually, a high gas velocity can result in an increased gas throughput. DMTO catalyst particles have similar physical properties as FCC catalyst, as will be addressed in the next section, and are typically type A particles according to Geldart's classification.[139] For this type of particle, a superficial gas velocity of 0.5−1.5 m/s would make the fluidized bed operating in the turbulent fluidized bed regime. An even higher superficial gas velocity will make the fluidized bed transit from turbulent fluidization to fast fluidization. A turbulent fluidized bed reactor offers apparent operational advantages over the bubbling and fast fluidized bed due to the excellent catalyst−gas contact, high mass transfer efficiency, and large solids holdup.[140] In the DMTO process, a turbulent fluidized bed reactor operating at a superficial gas velocity of 1−1.5 m/s is designed.

6.2. DMTO Fluidized Bed Reactor Scale-Up. The scale-up of a new fluidized bed process is rather an engineering practice than an exact science.[141−143] First, the fluidization behavior in the reactor can vary significantly when the physical properties (i.e., size and density) of catalyst particles are different.[139] Second, the hydrodynamics in the fluidized bed such as the gas bubbles, solid mixing and dispersion, and gas mixing and dispersion is closely related to the bed diameter as well as the operation conditions.[144,145] The dream of chemical engineers is to directly scale up the fluidized bed process by use of a reliable mathematical model.[141] Although great effort has been devoted to establish such a model[141] in recent years, the DMTO fluidized bed reactor was scaled up through the experiments at different scales.

6.2.1. Comparison between DMTO and FCC Process. The fluidized bed reactor−regenerator configuration in DMTO

process is very similar to that in the FCC process. We had made a detailed comparison between the DMTO and FCC process in terms of feedstock, reaction mechanism, catalyst, product, and process (see Table S1). The big difference is that in the FCC process, the reactor is a riser, while in DMTO, it is a turbulent fluidized bed. However, in the FCC process, the regenerator is operating in the turbulent fluidized bed regime. The experience in the design and operation of FCC turbulent fluidized bed regenerator can certainly help to reduce the risk of DMTO reactor scale-up. The good fluidization performance of FCC catalyst is well-known to chemical engineers for decades. The FCC catalyst is a type A particle according to Geldart's classification.[139] Therefore, it had been decided that the DMTO catalyst would be a type A particle and has similar physical properties as the FCC catalyst. Typical properties of DMTO catalyst are shown in Table 5. The two most important parameters, the particle size distribution and particle density, were specifically designed during the catalyst manufacturing. The percentage of fines less than 40 μm in the catalyst, which is critical for catalyst circulation, is maintained at 15%.

6.2.2. DMTO Reactor Scale-Up. To be sufficiently confident in designing a commercial DMTO reactor, the following problems have to be resolved: (1) fluidization of catalyst in methanol gas; (2) catalyst circulation; (3) catalyst stripping; (4) catalyst attrition; (5) optimal catalyst residence time; (6) optimal gas–catalyst contact time; (7) effect of reactor size on fluidization; (8) effect of reactor size on reaction; (9) heat of reaction.

Figure 15 shows the process of DMTO fluidized bed reactor scale-up. Table 6 summaries the typical operation conditions at
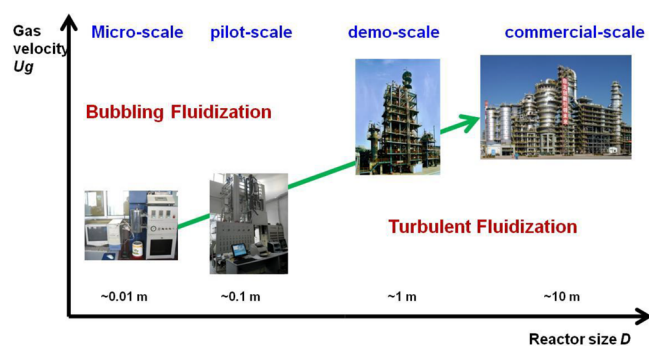

Figure 15. Scale up of DMTO fluidized bed reactor.

different scale. The microscale fluidized bed is a fixed fluidized bed operated at bubbling fluidization regime without catalyst circulation. In this stage, the main task is to evaluate performance of DMTO catalyst and investigate the optimal operation window. It was found that the coke content is nearly a linear function of catalyst residence time (RT). We determined the optimal catalyst RT in microscale fluidized bed reactor, which was consequently implemented into the design of pilot-scale fluidized bed reactor. Also the microscale

reactor was used to study the reaction kinetics of DMTO process. Pilot-scale reactor is connected to a fluidized bed regenerator via standpipes, thus a complete catalyst circulation between reactor and regenerator can be tested. The pilot-scale reactor was operated at bubbling fluidization regime, and the catalyst circulation rate was determined by the catalyst RT obtained from the microscale experiments. In the pilot-scale reactor, the catalyst stripping was also tested. The gas–catalyst contact time and WHSV were kept the same for both microscale and pilot-scale reactors, which are 2 to 3 s and 2–3 h^{-1}, respectively. The fluidization performance of DMTO catalyst was preliminarily demonstrated in the pilot-scale reactor. The methanol conversion is above 99% for both microscale and pilot-scale reactors. Typical selectivity (in nonaqueous products) to ethene and propene is 80% in both microscale reactor and pilot-scale reactor.

In the microscale and pilot-scale, the superficial gas velocity in the reactor is 1 to 20 cm/s, which lies in the bubbling fluidization regime. In the demonstration scale, the superficial gas velocity in the reactor was promoted to achieve a truly turbulent fluidization. In the demonstration unit, of particular importance is the high WHSV (∼5 h^{-1}) and superficial gas velocity (1∼1.5 m/s), which was significantly different from that in microscale and pilot-scale reactor. In addition to that, the catalyst circulation, stripping, attrition, as well as heat of reaction were carefully studied in the demonstration unit.

6.3. DMTO Demonstration Unit. In 2006, the DMTO demonstration scale unit was constructed in Huaxian, Shanxi. Figure 16 is the schematic flow diagram of the DMTO
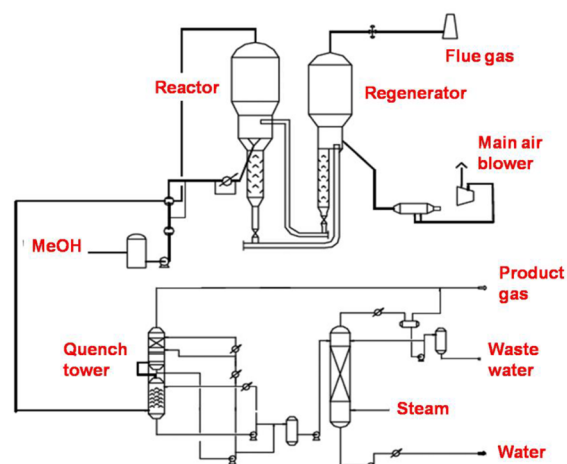

Figure 16. Schematic flow diagram of the DMTO demonstration unit.

demonstration unit. The unit consists of fluidized bed reactor, fluidized bed regenerator, quench tower, and sour water stripper. The aims of the demonstration unit are to study the hydrodynamics and reaction performance of DMTO turbulent fluidized bed reactor and provide data for commercial reactor design, in addition to get exact product distribution data

Table 6. Scale-Up of DMTO Fluidized Bed Reactor

	microscale	pilot-scale	demo-scale	commercial-scale
MeOH feed, kg/d	0.5	50	50 000	5 500 000
catalyst inventory, kg	0.01	1	400	45 000
superficial gas velocity, m/s	0.01∼0.1	0.01∼0.2	1∼2	1∼2
fluidization regime	bubbling	bubbling	turbulent	turbulent

including all trace amounts of impurities, such as oxygenates, alkynes and dienes, for the following olefin recovery unit design. The DMTO reactor in the demonstration unit has a diameter of 1 m, with a methanol feed rate of 2.5 t/h. The unit was running for a total of 1200 h. The influences of the operation conditions on methanol conversion and selectivity to ethene and propene were studied. Catalyst attrition was also tested in the demonstration unit. Figure 17 shows the results
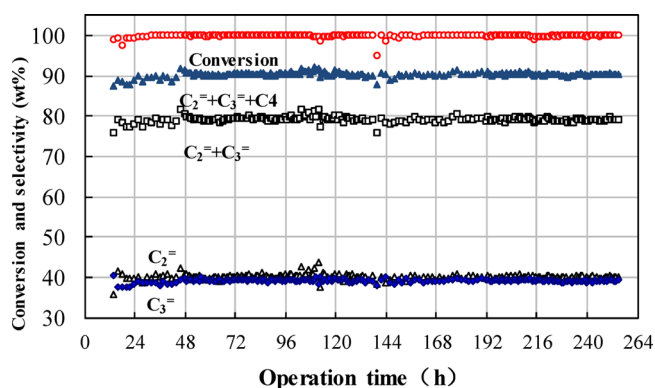
Figure 17. Reaction results in DMTO demonstration unit under continuous operation.

during continuous operation, and Table 7 summarizes the average reaction results. In the demonstration unit, the average selectivity to ethene and propene was 79.21%, and the methanol conversion was higher than 99%. Furthermore, the ethene/propene ratio could be adjusted in the range of 0.8 to 1.2 by varying operation conditions. The data from this demonstration unit was implemented in the design package of commercial DMTO units.

Table 7. Average Reaction Results in DMTO Demonstration Unit

|	unit	value
MeOH conversion	wt %	99.42
$C_2^= + C_3^=$ selectivity	wt %	79.21
$C_2^= + C_3^= + C_4^=$ selectivity	wt %	89.15
MeOH consumption	t MeOH/t ($C_2^= + C_3^=$)	2.96

6.4. Reaction Engineering Research for DMTO Process. DICP has carried out a series of reaction engineering research for DMTO process, which aims at understanding the fluidization of the DMTO catalyst, optimizing the DMTO reactor design, and improving the operation efficiency.

6.4.1. Fluidization of DMTO Catalyst. Although the fluidization of Geldart type A particles such as FCC catalyst has been subject of research for decades, the knowledge on fluidization of DMTO catalyst is quite poor. It was found[146] that the minimum fluidization velocity of DMTO catalyst measured in the laboratory is lower than that predicted by Abrahamsen and Geldart's empirical correlation,[147] which is widely used for FCC catalyst particles. Thus, a modified correlation for the minimum fluidization velocity of DMTO catalyst was proposed by Zhao et al.[146] An electrical capacitance tomography (ECT) method is being established to study the minimum bubbling velocity and the homogeneous fluidization of DMTO catalyst.[148]

Another work is to develop internals for DMTO reactor to control catalyst residence time distribution. As the catalyst residence time distribution is closely linked to the coke distribution in the reactor, which in turn affects the selectivity to light olefins in DMTO process. By use of KCl particles as tracers, we studied the influence of internals on catalyst residence time distribution in a pilot-scale cold flow fluidized bed. On the basis of the results, an optimal internal was developed, and this will be implemented in the large scale cold flow fluidization facility in DICP. To further optimize DMTO fluidized bed reactor, a multifunctional cold-flow fluidization facility has been constructed in DICP. This facility includes a turbulent fluidized bed (inner diameter of 1.5 m), a bubbling fluidized bed (inner diameter of 1m), and a riser (inner diameter of 30 cm, and length of 15 m).

6.4.2. Attrition of DMTO Catalyst. Some fundamental research has been performed to study the attrition of the DMTO catalyst. It has been found that the DMTO catalyst is better than the typical FCC catalyst in the market in terms of attrition resistance. Essentially, the attrition mechanisms in different operation regimes inside the DMTO reactor were studied in the laboratory. Particularly, the focus is the attrition in the reaction conditions. Our results showed that the attrition mechanism of the DMTO catalyst at room temperature is different from that at high temperature. At room temperature, both fragmentation and abrasion occur, although at high temperature of 500 °C, the abrasion is dominant.[149] This means an optimal design of dust recovering system to capture superfine particles (less than 5 μm) might be essential.

6.4.3. DMTO Reactor Model. A reactor modeling approach, including hydrodynamics[150] and kinetics,[151,152] is being established to simulate the DMTO fluidized bed reactor. The hydrodynamics of the DMTO reactor in the demonstration unit was simulated by use of an EMMS-based two-fluid CFD model (Figure 18). The results were compared with the
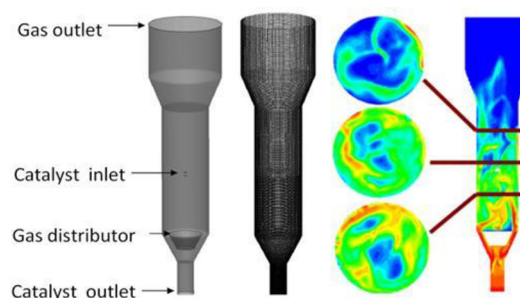
Figure 18. CFD simulation of the DMTO fluidized bed reactor in the demonstration unit.

experimental data, and the solid fraction profile along the axial direction show a good agreement.[150] A lumped kinetic model for industrial DMTO catalyst was simultaneously developed based on microscale reactor experiments.[151,152] The kinetic model can predicted the experimental data in the pilot-scale DMTO reactor reasonably well. Via a collaboration with Prof. Jinghai Li's group in Institute of Process Engineering, Chinese Academy of Sciences, we are developing a comprehensive reactor model for industrial DMTO fluidized bed reactor.

6.5. DMTO Commercial Units. In May 2010, the world's first DMTO commercial unit was constructed in Baotou, North China by Shenhua group (Figure 19). The capacity of the unit is to produce 0.6 Mt polyethylene and polypropylene per year.

Figure 19. DMTO commercial unit in Shenhua Baotou.

Figure 21. Methanol conversion and light olefins selectivity in commercial DMTO unit.

The reactor is a shallow turbulent fluidized bed with a diameter of 11 m and bed height of 3 m. Some engineering challenges such as solid–gas distribution, catalyst mixing, and gas breakthrough have to be solved in the design of this large shallow fluidized bed. In August 2010, the unit was successfully started up. A method to start up the unit by use of the heat released from DMTO reactor was proposed. Compared to FCC process, this method can significantly reduce the time for start up.[153] Figure 20 shows the change of temperature in the
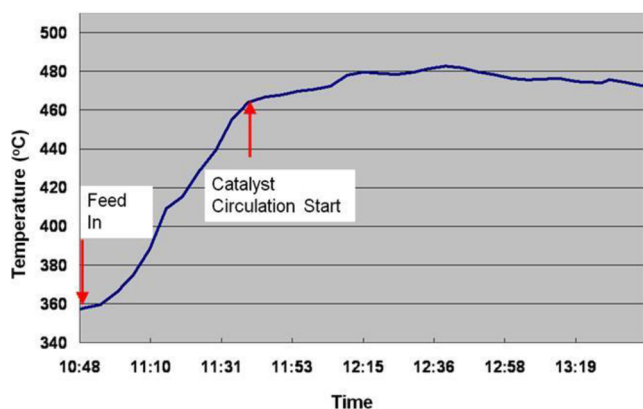

Figure 20. Temperature increase in commercial DMTO reactor during start up.

DMTO reactor during start up. As can be seen, the reactor temperature can rise by 100 °C in 60 min. When the reactor was heated to 460 °C, the catalyst started to circulate between the reactor and regenerator. It is worthy to note that fundamental research on catalyst deactivation at low temperature (see Section 3.3) gave important information for the development of the start-up method. According to the research, there is a fast deactivation of the catalyst at lower temperature range (300−350 °C), and the catalyst should avoid this deactivation. Furthermore, circulation of catalyst should not start until a high reaction temperature and high methanol conversion is achieved.

Figure 21 is the methanol conversion and selectivity to light olefins for the commercial unit, which are measured by the online gas chromatography (GC). The methanol conversion is 100%, and the selectivity is higher than 80%. The selectivity is better than the results in pilot-scale and demo-scale units,
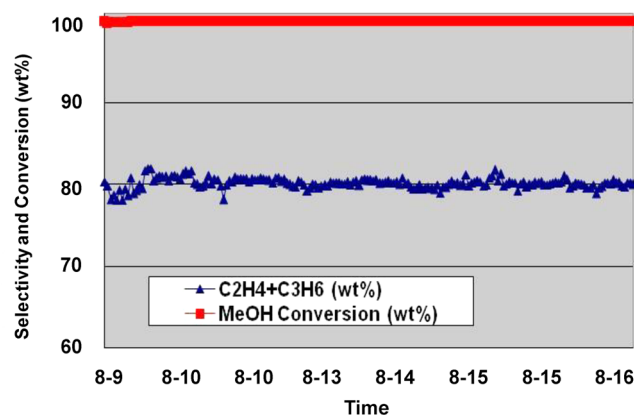
which may be due to the good fluidization in commercial DMTO reactor. In March 2011, a 72 h performance test was carried out for the Shenhua Baotou DMTO unit. On the basis of the test data, the methanol consumption is 2.96 tons per ton product of ethene and propene, which is the same as in the demonstration unit. Up to now, this plant has produced more than 2.1 million tons of polyolefins.

6.6. DMTO-II Process. After the success of DMTO process, DICP developed the second generation DMTO process (DMTO-II), in which the byproduct of C_4^+ was separated from the product stream and further converted to ethene and propene in a second cracking fluidized bed reactor. Figure 22
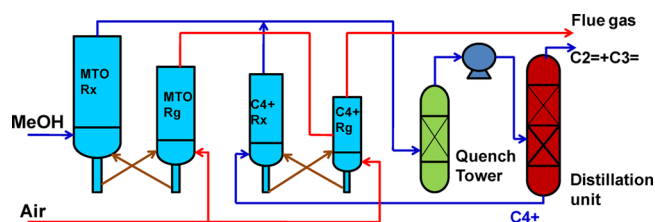

Figure 22. Scheme of DMTO-II process.

shows the scheme of DMTO-II process. The main feature of DMTO-II is that the MTO reaction and C_4^+ conversion reaction share the same catalyst and could use one regenerator for catalyst regeneration. In 2009, the DMTO demonstration unit was revamped by adding a second bubbling fluidized bed reactor for C_4^+ cracking. From 2009 to 2010, the DMTO-II process had been verified in the demonstration unit. The results obtained from the demonstration unit are listed in Table 8. As can be seen, the selectivity to ethene and propene increased from 79.21% in DMTO process to 85.68% in the DMTO-II process with 60 wt % of C_4^+ recycling, and the methanol consumption for producing one ton ethene and propene reduced from 2.96 to 2.67 tons. This apparently improves the economic profits for DMTO process. In October 26, 2010,

Table 8. Average Results of DMTO-II Demonstration Unit

	unit	value
MeOH conversion	%	99.97
$C_2^=+C_3^=$ selectivity	wt %	85.68
MeOH consumption	t MeOH/t ($C_2^=$ + $C_3^=$)	2.67
$C_2^=/C_3^=$ ratio		0.7−1.1

DICP licensed the first DMTO-II unit (0.67 Mt/a polyethylene and polypropylene product) to Pucheng Clean Energy Chemical Co. Ltd. In December 22, 2014, the first commercial DMTO-II unit was successfully started up.

6.7. DMTO in China. Since 2006, DICP started to license DMTO technology worldwide. Until December 31st, 2014, in total 20 licenses were approved with a total capacity of 11 Mt/a ethene and propene production. Six commercial DMTO units and one commercial DMTO-II unit have been put into stream with olefins production capacity exceeding 4 Mt/a. More than 10 units will be commissioned in near future according to the plan. It is expected that MTO will become an important alternative to traditional light olefins' production technology such as steam cracking of naphtha.

7. SUMMARY AND OUTLOOK

(1) MTO is an interesting and important reaction for both fundamental research and industrial applications. Our mechanism studies tend to prove that the HCP mechanism is generally effective for the reaction; however, the carbenium ions vary with the cavity size. Besides pore opening size of molecular sieves, the cavity seems to control selectivity as well. Although a reaction network was proposed, there still remain many scientific challenges, such as how the first C−C bond forms, what happens in the induction period, what are the exact relations among different reaction routes, how coke forms, and how to control coking reaction in the reaction network, among others. A better understanding of the MTO reaction is certainly critical for further improving the DMTO technology.

(2) Fundamental investigations on the SAPO molecular sieve synthesis offered strong support to the catalyst development. The successful development of the DMTO catalyst suggests that many essential issues need to be solved for a commercial applicable catalyst. The opportunities for further MTO catalyst innovation include the crystallization mechanism studies for precise control of synthesis, as well as the application of new catalytic materials such as meso-microporous zeolites that have been confirmed with longer lifetime for many reactions. To find a molecular sieve with suitable cavity size restricting coke formation is also a potential direction for developing a better MTO catalyst.

(3) The development of DMTO technology is an integration of many new analyses, including catalyst and engineering aspects. The strategy to design DMTO catalyst with similar physical properties (density, particle size distribution, etc.) to FCC catalyst, enabling the application of industrial FCC research, operation, and design experience into the process development, is also critical for the rapid scale-up of DMTO reactor through demonstration test to commercialization.

(4) DMTO technology has been well developed and demonstrated in China, which led to the successful construction and commissioning of the world's first coal to olefin plant. The application of DMTO technology is expected to change the strategy and framework for the supply of olefins in China. It can also play an important role in other countries abundant in coal or natural gas.

ASSOCIATED CONTENT

Ⓢ Supporting Information
The following file is available free of charge on the ACS Publications website at DOI: 10.1021/acscatal.5b00007.

> Detailed comparison between DMTO and FCC process (PDF)

AUTHOR INFORMATION

Corresponding Author
*E-mail: liuzm@dicp.ac.cn. Tel.: 0086-411-84379998.
Notes
The authors declare no competing financial interest.

REFERENCES

(1) Chang, C. D.; Silvestri, A. J. *J. Catal.* **1977**, *47*, 249−259.
(2) Stocker, M. *Microporous Mesoporous Mater.* **1999**, *29*, 3−48.
(3) Wang, W.; Hunger, M. *Acc. Chem. Res.* **2008**, *41*, 895−904.
(4) Haw, J. F.; Song, W. G.; Marcus, D. M.; Nicholas, J. B. *Acc. Chem. Res.* **2003**, *36*, 317−326.
(5) Arstad, B.; Kolboe, S. *J. Am. Chem. Soc.* **2001**, *123*, 8137−8138.
(6) Chen, D.; Moljord, K.; Holmen, A. *Microporous Mesoporous Mater.* **2012**, *164*, 239−250.
(7) Svelle, S.; Joensen, F.; Nerlov, J.; Olsbye, U.; Lillerud, K.-P.; Kolboe, S.; Bjorgen, M. *J. Am. Chem. Soc.* **2006**, *128*, 14770−14771.
(8) Bjorgen, M.; Akyalcin, S.; Olsbye, U.; Benard, S.; Kolboe, S.; Svelle, S. *J. Catal.* **2010**, *275*, 170−180.
(9) Bjorgen, M.; Olsbye, U.; Petersen, D.; Kolboe, S. *J. Catal.* **2004**, *221*, 1−10.
(10) Dai, W.; Wang, X.; Wu, G.; Guan, N.; Hunger, M.; Li, L. *ACS Catal.* **2011**, *1*, 292−299.
(11) Cao, G.; Matu J. S. U.S. Patent 6,680,278, Jan. 20, 2004.
(12) Chang, Y.; Vaughn, S. N.; Martens, L. R. M. U.S. Patent 7,271,123, Sep. 18, 2007.
(13) Mertens, M.; Strohmaier, K. G. U.S. Patent 6,773,688, Aug. 10, 2004.
(14) Liu, G.; Tian, P.; Liu, Z. *HuaXueJinZhan* **2010**, *22*, 1531−1537.
(15) Wilson, S.; Barger, P. *Microporous Mesoporous Mater.* **1999**, *29*, 117−126.
(16) Vora, B. V.; Marker, T. L.; Barger, P. T.; Nilsen, H. R.; Kvisle, S.; Fuglerud, T. *Stud. Surf. Sci. Catal.* **1997**, *107*, 87−98.
(17) Chen, J. Q.; Bozzano, A.; Glover, B.; Fuglerud, T.; Kvisle, S. *Catal. Today* **2005**, *106*, 103−107.
(18) Coute, N. P.; Kuechler, K. H.; Chisholm, P. N.; Vaughn, S. N.; Lattner, J. R.; Kuechler Sr., W. L. U.S. Patent 6,673,978, Jan. 6, 2004.
(19) Koempel, H.; Liebner, W. *Stud. Surf. Sci. Catal.* **2007**, *167*, 261−267.
(20) Olsbye, U.; Svelle, S.; Bjorgen, M.; Beato, P.; Janssens, T. V. W.; Joensen, F.; Bordiga, S.; Lillerud, K. P. *Angew. Chem., Int. Ed.* **2012**, *51*, 5810−5831.
(21) Liu, Z.; Liang, J. *Curr. Opin. Solid State Mater. Sci.* **1999**, *4*, 80−84.
(22) Liu, Z.; Sun, C.; Wang, G.; Wang, Q.; Cai, G. *Fuel Process. Technol.* **2000**, *62*, 161−172.

(23) Chen, N. Y.; Reagan, W. J. *J. Catal.* **1979**, *59*, 123−129.

(24) Ono, Y.; Mori, T. *J. Chem. Soc. Fara. Trans. I* **1981**, *77*, 2209−2221.

(25) Chang, C. D. *Catal. Rev.* **1983**, *25*, 1−118.

(26) Swabb, E. A.; Gates, B. C. *Ind. Eng. Chem. Fundam.* **1972**, *11*, 540−545.

(27) Hutchings, G. J.; Gottschalk, F.; Hall, M. V. M; Hunter, R. *J. Chem. Soc. Fara. Trans. I* **1987**, *83*, 571−583.

(28) Olah, G. A. *Pure Appl. Chem.* **1981**, *53*, 201−207.

(29) Kagi, D. *J. Catal.* **1981**, *69*, 242−243.

(30) Clarke, J. K. A.; Darcy, R.; Hegarty, B. F.; Odonoghue, E.; Amirebrahimi, V.; Rooney, J. J. *J. Chem. Soc., Chem. Commun.* **1986**, 425−426.

(31) Zatorski, W.; Kryzanowski, S. *Acta Phys. Chem.* **1977**, *24*, 347−352.

(32) Dessau, R. M. *J. Catal.* **1986**, *99*, 111−116.

(33) Dessau, R. M.; Lapierre, R. B. *J. Catal.* **1982**, *78*, 136−141.

(34) Mole, T.; Bett, G.; Seddon, D. *J. Catal.* **1983**, *84*, 435−445.

(35) Mole, T.; Whiteside, J. A.; Seddon, D. *J. Catal.* **1983**, *82*, 261−266.

(36) Dahl, I. M.; Kolboe, S. *Catal. Lett.* **1993**, *20*, 329−336.

(37) Dahl, I. M.; Kolboe, S. *J. Catal.* **1994**, *149*, 458−464.

(38) Dahl, I. M.; Kolboe, S. *J. Catal.* **1996**, *161*, 304−309.

(39) Hunger, M. *Catal. Rev.* **1997**, *39*, 345−393.

(40) Wang, W.; Jiang, Y. J.; Hunger, M. *Catal. Today* **2006**, *113*, 102.

(41) Xu, T.; White, J. L. U.S. Patent 6,743,747, Jun. 1, 2004.

(42) Xu, T.; White, J. L. U.S. patent 6,734,330, May 11, 2004.

(43) Arstad, B.; Kolboe, S. *Catal. Lett.* **2001**, *71*, 209−212.

(44) Fu, H.; Song, W. G.; Haw, J. F. *Catal. Lett.* **2001**, *76*, 89−94.

(45) Haw, J. F.; Marcus, D. M. *Top. Catal.* **2005**, *34*, 41−48.

(46) Song, W. G.; Fu, H.; Haw, J. F. *J. Am. Chem. Soc.* **2001**, *123*, 4749−4754.

(47) Song, W. G.; Fu, H.; Haw, J. F. *J. Phys. Chem. B* **2001**, *105*, 12839−12843.

(48) Song, W. G.; Haw, J. F.; Nicholas, J. B.; Heneghan, C. S. *J. Am. Chem. Soc.* **2000**, *122*, 10726−10727.

(49) Haw, J. F.; Nicholas, J. B.; Song, W. G.; Deng, F.; Wang, Z. K.; Xu, T.; Heneghan, C. S. *J. Am. Chem. Soc.* **2000**, *122*, 4763−4774.

(50) Song, W. G.; Nicholas, J. B.; Sassi, A.; Haw, J. F. *Catal. Lett.* **2002**, *81*, 49−53.

(51) Xu, T.; Barich, D. H.; Goguen, P. W.; Song, W. G.; Wang, Z. K.; Nicholas, J. B.; Haw, J. F. *J. Am. Chem. Soc.* **1998**, *120*, 4025−4026.

(52) Xu, T.; Haw, J. F. *J. Am. Chem. Soc.* **1994**, *116*, 10188−10195.

(53) Wang, C.; Chu, Y. Y.; Zheng, A. M.; Xu, J.; Wang, Q.; Gao, P.; Qi, G. D.; Gong, Y. J.; Deng, F. *Chem.- Eur. J.* **2014**, *20*, 12432−12443.

(54) Sassi, A.; Wildman, M. A.; Ahn, H. J.; Prasad, P.; Nicholas, J. B.; Haw, J. F. *J. Phys. Chem. B* **2002**, *106*, 2294−2303.

(55) Sassi, A.; Wildman, M. A.; Haw, J. F. *J. Phys. Chem. B* **2002**, *106*, 8768−8773.

(56) Arstad, B.; Nicholas, J. B.; Haw, J. F. *J. Am. Chem. Soc.* **2004**, *126*, 2991−3001.

(57) Bjorgen, M.; Bonino, F.; Kolboe, S.; Lillerud, K. P.; Zecchina, A.; Bordiga, S. *J. Am. Chem. Soc.* **2003**, *125*, 15863−15868.

(58) McCann, D. M.; Lesthaeghe, D.; Kletnieks, P. W.; Guenther, D. R.; Hayman, M. J.; Van Speybroeck, V.; Waroquier, M.; Haw, J. F. *Angew. Chem., Int. Ed.* **2008**, *47*, 5179−5182.

(59) Nicholas, J. B.; Haw, J. F. *J. Am. Chem. Soc.* **1998**, *120*, 11804−11805.

(60) Bjorgen, M.; Svelle, S.; Joensen, F.; Nerlov, J.; Kolboe, S.; Bonino, F.; Palumbo, L.; Bordiga, S.; Olsbye, U. *J. Catal.* **2007**, *249*, 195−207.

(61) Svelle, S.; Olsbye, U.; Joensen, F.; Bjorgen, M. *J. Phys. Chem. C* **2007**, *111*, 17981−17984.

(62) Guisnet, M.; Costa, L.; Ribeiro, F. R. *J. Mol. Catal. A: Chem.* **2009**, *305*, 69−83.

(63) Liu, Z.; Qi, Y. *Bull. Chin. Acad. Sci.* **2006**, *21*, 406−408.

(64) Li, J. Ph.D. Dissertation, Dalian Institute of Chemical Physics, 2008.

(65) Li, J.; Qi, Y.; Liu, Z.; Liu, G.; Chang, F. *Chin. J. Catal.* **2008**, *29*, 660−664.

(66) Li, J.; Qi, Y.; Liu, Z.; Liu, G.; Zhang, D. *Catal. Lett.* **2008**, *121*, 303−310.

(67) Li, J.; Qi, Y.; Xu, L.; Liu, G.; Meng, S.; Li, B.; Li, M.; Liu, Z. *Catal. Commun.* **2008**, *9*, 2515−2519.

(68) Li, J.; Wei, Y.; Liu, G.; Qi, Y.; Tian, P.; Li, B.; He, Y.; Liu, Z. *Catal. Today* **2011**, *171*, 221−228.

(69) Wang, C.; Wang, Y.; Xie, Z.; Liu, Z. *J. Phys. Chem. C* **2009**, *113*, 4584−4591.

(70) Su, X.; Tian, P.; Fan, D.; Xia, Q.; Yang, Y.; Xu, S.; Zhang, L.; Zhang, Y.; Wang, D.; Liu, Z. *ChemSusChem* **2013**, *6*, 911−918.

(71) Su, X.; Tian, P.; Li, J.; Zhang, Y.; Meng, S.; He, Y.; Fan, D.; Liu, Z. *Microporous Mesoporous Mater.* **2011**, *144*, 113−119.

(72) Tian, P.; Su, X.; Wang, Y.; Xia, Q.; Zhang, Y.; Fan, D.; Meng, S.; Liu, Z. *Chem. Mater.* **2011**, *23*, 1406−1413.

(73) Li, J.; Wei, Y.; Chen, J.; Tian, P.; Su, X.; Xu, S.; Qi, Y.; Wang, Q.; Zhou, Y.; He, Y.; Liu, Z. *J. Am. Chem. Soc.* **2012**, *134*, 836−839.

(74) Li, J.; Wei, Y.; Xu, S.; Tian, P.; Chen, J.; Liu, Z. *Catal. Today* **2014**, *226*, 47−51.

(75) Xu, S.; Zheng, A.; Wei, Y.; Chen, J.; Li, J.; Chu, Y.; Zhang, M.; Wang, Q.; Zhou, Y.; Wang, J.; Deng, F.; Liu, Z. *Angew. Chem., Int. Ed.* **2013**, *52*, 11564−11568.

(76) Chen, J.; Li, J.; Wei, Y.; Yuan, C.; Li, B.; Xu, S.; Zhou, Y.; Wang, J.; Zhang, M.; Liu, Z. *Catal. Commun.* **2014**, *46*, 36−40.

(77) Li, J.; Wei, Y.; Chen, J.; Xu, S.; Tian, P.; Yang, X.; Li, B.; Wang, J.; Liu, Z. M. *ACS Catal.* **2014**, *5*, 661−665.

(78) Yuan, C.; Wei, Y.; Li, J.; Xu, S.; Chen, J.; Zhou, Y.; Wang, Q.; Xu, L.; Liu, Z. *Chin. J. Catal.* **2012**, *33*, 367−374.

(79) Wei, Y.; Li, J.; Yuan, C.; Xu, S.; Zhou, Y.; Chen, J.; Wang, Q.; Zhang, Q.; Liu, Z. *Chem. Commun.* **2012**, *48*, 3082−3084.

(80) Wei, Y.; Yuan, C.; Li, J.; Xu, S.; Zhou, Y.; Chen, J.; Wang, Q.; Xu, L.; Qi, Y.; Zhang, Q.; Liu, Z. *ChemSusChem* **2012**, *5*, 906−912.

(81) Yuan, C.; Wei, Y.; Xu, L.; Li, J.; Xu, S.; Zhou, Y.; Chen, J.; Wang, Q.; Liu, Z. *Chin. J. Catal.* **2012**, *33*, 768−770.

(82) Chen, J.; Li, J.; Yuan, C.; Xu, S.; Wei, Y.; Wang, Q.; Zhou, Y.; Wang, J.; Zhang, M.; He, Y.; Xu, S.; Liu, Z. *Catal. Sci. Technol.* **2014**, *4*, 3268−3277.

(83) Brent, M. L.; Celeste, A. M.; Robert, L. P.; Richard, T. G.; Thomas, R. C.; Edith, M. F. U.S. Patent 4,440,871, Apr. 3, 1984.

(84) Brent, M. L.; Celeste, A. M.; R. Lyle, P.; Richard, T. G.; Thomas, R. C.; Edith, M. F. *J. Am. Chem. Soc.* **1984**, *106*, 6092−6093.

(85) Liang, J.; Li, H. Y.; Zhao, S.; Guo, W. G.; Wang, R. H.; Ying, M. L. *Appl. Catal.* **1990**, *64*, 31−40.

(86) Chen, D.; Moljord, K.; Fuglerud, T.; Holmen, A. *Microporous Mesoporous Mater.* **1999**, *29*, 191−203.

(87) Vomscheid, R.; Briend, M.; Peltre, M. J.; Man, P. P.; Barthomeuf, D. *J. Phys. Chem.* **1994**, *98*, 9614−9618.

(88) Briend, M.; Vomscheid, R.; Peltre, M. J.; Man, P. P.; Barthomeuf, D. *J. Phys. Chem.* **1995**, *99*, 8270−8276.

(89) Sastre, G.; Lewis, D. W.; Catlow, C. R. A. *J. Phys. Chem.* **1996**, *100*, 6722−6730.

(90) Bleken, F.; Bjørgen, M.; Palumbo, L.; Bordiga, S.; Svelle, S.; Lillerud, K.-P.; Olsbye, U. *Top. Catal.* **2009**, *52*, 218−228.

(91) Xi, D.; Sun, Q.; Xu, J.; Cho, M.; Cho, H. S.; Asahina, S.; Li, Y.; Deng, F.; Terasaki, O.; Yu, J. *J. Mater. Chem. A* **2014**, *2*, 17994−18004.

(92) Dargahi, M.; Kazemian, H.; Soltanieh, M.; Rohani, S.; Hosseinpour, M. *Particuology* **2011**, *9*, 452−457.

(93) Vistad, Ø. B.; Akporiaye, D. E.; Taulelle, F.; Lillerud, K. P. *Chem. Mater.* **2003**, *15*, 1639−1649.

(94) Martins, G. A. V.; Berlier, G.; Coluccia, S.; Pastore, H. O.; Superti, G. B.; Gatti, G.; Marchese, L. *J. Phys. Chem. C* **2006**, *111*, 330−339.

(95) Wu, X.; Abraha, M. G.; Anthony, R. G. *Appl. Catal., A* **2007**, *260*, 63−69.

(96) Nishiyama, N.; Kawaguchi, M.; Hirota, Y.; Van Vu, D.; Egashira, Y.; Ueyama, K. *Appl. Catal., A* **2009**, *362*, 193−199.

(97) Buchholz, A.; Wang, W.; Arnold, A.; Xu, M.; Hunger, M. *Microporous Mesoporous Mater.* **2003**, *57*, 157−168.

(98) Hirota, Y.; Murata, K.; Miyamoto, M.; Egashira, Y.; Nishiyama, N. *Catal. Lett.* **2010**, *140*, 22−26.

(99) Zhang, L.; Bates, J.; Chen, D.; Nie, H. Y.; Huang, Y. *J. Phys. Chem. C* **2011**, *115*, 22309−22319.

(100) Li, Z.; Martinez-Triguero, J.; Concepcion, P.; Yu, J.; Corma, A. *Phys. Chem. Chem. Phys.* **2013**, *15*, 14670−14680.

(101) Li, H.; Liang, J.; Wang, R.; Liu, Z.; Zhao, S. *Petrochem. Technol.* **1987**, *16*, 340−346.

(102) Liu, Z.; Huang, X.; He, C.; Yang, Y.; Yang, L.; Cai, G. *Chin. J. Catal.* **1996**, *17*, 540−543.

(103) Liu, Z.; Sun, C.; Xu, L.; Yang, L.; Tian, P.; Tan, J. CN Patent 1131845C, Dec. 24, 2003.

(104) Liu, Z.; Xu, L.; Tian, P.; Yang, Y.; Yang, L.; He, C.; Lv, Z.; Meng, S.; Wang, G.; Sun, X.; Yang, H.; Wang, X.; Yuan, C.; Li, M.; Wei, Y.; Qi, Y.; Zhu, S.; Zhang, J.; Lu, X.; Wang, H.; Xie, P.; Li, B. CN Patent 100584758C, Jan. 27, 2010.

(105) Liu, Z.; Cai, G.; He, C.; Yang, L.; Wang, Z.; Luo, J.; Chang, Y.; Shi, R.; Jiang, Z.; Sun, C. CN Patent 1037334C, Feb. 11, 1998.

(106) Tan, J. Mater Dissertation, Dalian Institute of Chemical Physics, 1999.

(107) Du, A. Mater Dissertation, Dalian Institute of Chemical Physics, 2004.

(108) Zhang, D. Ph.D. Dissertation, Dalian Institute of Chemical Physics, 2007.

(109) Liu, G. Ph.D. Dissertation, Dalian Institute of Chemical Physics, 2008.

(110) Tan, J.; Liu, Z. M.; Bao, X. H.; Liu, X. C.; Han, X. W.; He, C. Q.; Zhai, R. S. *Microporous Mesoporous Mater.* **2002**, *53*, 97−108.

(111) Tian, P.; Li, B.; Xu, S.; Su, X.; Wang, D.; Zhang, L.; Fan, D.; Qi, Y.; Liu, Z. *J. Phys. Chem. C* **2013**, *117*, 4048−4056.

(112) Li, B.; Tian, P.; Qi, Y.; Zhang, L.; Xu, S.; Su, X.; Fan, D.; Liu, Z. *Chin. J. Catal.* **2013**, *34*, 593−603.

(113) Liu, G. Y.; Tian, P.; Zhang, Y.; Li, J. Z.; Xu, L.; Meng, S. H.; Liu, Z. M. *Microporous Mesoporous Mater.* **2008**, *111*, 143−149.

(114) Tian, P.; Liu, Z. M.; Xu, l.; Sun, C. *Stud. Surf. Sci. Catal.* **2001**, *135*, 248−248.

(115) Xu, L.; Liu, Z. M.; Tian, P.; Wei, Y.; Sun, C.; Li, S. *Stud. Surf. Sci. Catal.* **2001**, *135*, 247−247.

(116) Xu, L.; Liu, Z. M.; Du, A. P.; Wei, Y. X.; Sun, Z. G. *Stud. Surf. Sci. Catal.* **2004**, *147*, 445−450.

(117) Liu, Z.; Xu, L.; Sun, C.; Huang, T.; Tian, P.; Yang, L.; Tan, J. EP Patent 1,142,833, July 10, 2009.

(118) Liu, G. Y.; Tian, P.; Li, J. Z.; Zhang, D. Z.; Zhou, F.; Liu, Z. M. *Microporous Mesoporous Mater.* **2008**, *114*, 416−423.

(119) Barthomeuf, D. *Zeolites* **1994**, *14*, 394−401.

(120) Mores, D.; Stavitski, E.; Kox, M. H.; Kornatowski, J.; Olsbye, U.; Weckhuysen, B. M. *Chem. − Eur. J.* **2008**, *14*, 11320−11327.

(121) Liu, G.; Tian, P.; Zhang, Y.; Li, J.; Xu, L.; Meng, S.; Liu, Z. *Microporous Mesoporous Mater.* **2008**, *111*, 143−149.

(122) Izadbakhsh, A.; Farhadi, F.; Khorasheh, F.; Sahebdelfar, S.; Asadi, M.; Yan, Z. F. *Microporous Mesoporous Mater.* **2009**, *126*, 1−7.

(123) Xu, L.; Du, A.; Wei, Y.; Meng, S.; He, Y.; wang, Y.; Yu, Z.; Zhang, X.; Liu, Z. *Chin. J. Catal.* **2008**, *29*, 727−732.

(124) Fan, D.; Tian, P.; Xu, S.; Xia, Q.; Su, X.; Zhang, L.; Zhang, Y.; He, Y.; Liu, Z. *J. Mater. Chem.* **2012**, *22*, 6568−6574.

(125) Fan, D.; Tian, P.; Su, X.; Yuan, Y.; Wang, D.; Wang, C.; Yang, M.; Wang, L.; Xu, S.; Liu, Z. *J. Mater. Chem. A* **2013**, *1*, 14206−14213.

(126) Wang, D.; Tian, P.; Yang, M.; Xu, S.; Fan, D.; Su, X.; Yang, Y.; Wang, C.; Liu, Z. *Microporous Mesoporous Mater.* **2014**, *194*, 8−14.

(127) van Heyden, H.; Mintova, S.; Bein, T. *Chem. Mater.* **2008**, *20*, 2956−2963.

(128) Zhu, J.; Cui, Y.; Wang, Y.; Wei, F. *Chem. Commun.* **2009**, 3282−3284.

(129) Yang, H.; Liu, Z.; Gao, H.; Xie, Z. *J. Mater. Chem.* **2010**, *20*, 3227−3231.

(130) Schmidt, F.; Paasch, S.; Brunner, E.; Kaskel, S. *Microporous Mesoporous Mater.* **2012**, *164*, 214−221.

(131) Sun, Q.; Wang, N.; Xi, D.; Yang, M.; Yu, J. *Chem. Commun.* **2014**, *50*, 6502−6505.

(132) Hirota, Y.; Murata, K.; Tanaka, S.; Nishiyama, N.; Egashira, Y.; Ueyama, K. *Mater. Chem. Phys.* **2010**, *123*, 507−509.

(133) Yang, M.; Tian, P.; Wang, C.; Yuan, Y.; Yang, Y.; Xu, S.; He, Y.; Liu, Z. *Chem. Commun.* **2014**, *50*, 1845−1847.

(134) Wang, C.; Yang, M.; Tian, P.; Xu, S.; Yang, Y.; Wang, D.; Yuan, Y.; Liu, Z. *J. Mater. Chem. A* **2015**, accepted.

(135) Liu, Z.; Tian, P.; Xu, L.; Yang, L.; Lv, Z.; Qi, Y.; He, C.; Wei, Y.; Zhang, J.; Meng, S.; Li, M.; Yuan, C.; Wang, X.; Yang, Y.; Lu, X.; Zhu, S.; Xie, P.; Sun, X.; Yang, H.; Wang, H.; Li, B. CN Patent 101122145C, Oct. 20, 2010.

(136) Tian, P.; Liu, Z.; Xu, L.; Yang, L.; Qi, Y.; Wang, X.; Yuan, C.; Lv, Z.; Meng, S. CN Patent 101121146B, Sep. 14, 2011.

(137) Tian, P.; Liu, Z.; Xu, L.; Sang, S.; He, C.; Yang, L.; Yuan, C. CN Patent 101157057B, Dec. 1, 2010.

(138) Miller, L. W. U.S. Patent 6,166,282, Dec. 26, 2000.

(139) Geldart, D. *Powder Technol.* **1973**, *7*, 285−292.

(140) Du, B.; Fan, L.; Wei, F.; Warsito, W. *AIChE J.* **2002**, *48*, 1896−1909.

(141) Knowlton, T. M.; Karri, S. B. R.; Issangya, A. *Powder Technol.* **2005**, *150*, 72−77.

(142) Matsen, J. M. *Powder Technol.* **1996**, *88*, 237−244.

(143) Rüdisüli, M.; Schildhauera, T. J.; Biollaz, S. M. A.; van Ommen, J. R. *Powder Technol.* **2012**, *217*, 21−38.

(144) Gauthier, T. A. *Int. J. Chem. Reactor Eng.* **2009**, *7*, A22.

(145) Werther, J. *AIChE symposium series* **1974**, *70*, 53−62.

(146) Zhao, Y.; Hao, J.; Ye, M.; Liu, Z. Proceedings of the 11th International Conference on Fluidized Bed Technology (CFB-11), Beijing, Chian, May 14−17, 2014; Li, J. H., Eds; Chemical Industry Press: Beijing, 2014.

(147) Abrahamsen, A. R.; Geldart, D. *Powder Technol.* **1980**, *26*, 35−46.

(148) Luo, Q.; Zhao, Y.; Ye, M.; Liu, Z. *CIESC Journal* **2014**, *65*, 2504−2512.

(149) Ying, L.; Ye, M.; Cheng, Y.; Li, X.; Liu, Z. Proceedings of the 14th International Conference on Fluidization, Noordwijkerhout, Netherlands, May 26-31, 2013; Kuipers, J. A. M.; Mudde, R. F.; van Ommen, J. R., Deen, N. G., Eds; ECI Symposium Series, 2013.

(150) Hao, J.; Zhao, Y.; Ye, M.; Liu, Z. *Adv. Powder Technol.* **2015**, in revision.

(151) Zhao, Y.; Li, H.; Ye, M.; Liu, Z. *Ind. Eng. Chem. Res.* **2013**, *52*, 11354−11364.

(152) Ying, L.; Ye, M.; Cheng, Y.; Li, H.; Liu, Z. *Chem. Eng. Res. Des.* Submitted for publication, 2015.

(153) Liu, Z.; Lv, Z.; He, C.; Liu, Y.; Qi, Y.; Min, X.; Wang, G.; Wang, X.; Zhang, J. CN Patent 101130466B, May 4, 2011.